CHAPTER 3:

INTRODUCTION TO THE NOx ABATEMENT PROCESS AT RFAAP AND COMPUTER SIMULATION OF THE NOx ABATEMENT PROCESS AS A CONVERSION-REACTION MODEL

3.1 Introduction

3.1.1 An Overview

This chapter introduces the reader to a specific application, or case study, of NOx removal technology, that being the NOx abatement system installed at the Radford Facility and Army Ammunition Plant (RFAAP), Radford, Virginia. The system at RFAAP reduces NOx emissions from fumes emanating from the cellulose nitration reactors at the site. Two major components make up the continuous NOx abatement system. A scrubber/absorber tower contacts the NOx-laden fumes with water, producing nitric acid from the aqueous absorption of NOx gases. Downstream of the scrubber/absorber tower, a reaction vessel with a honeycomb-structured heterogeneous catalyst bed reduces NOx with ammonia to atmospheric nitrogen and water. We give a brief summary of the reaction chemistry occurring in these two units as proposed by Radford.

Further, we introduce the trial-and-error method by which we plan to achieve an accurate working computer model for exploring system behavior and design optimization. We present an ASPEN Plus computer simulation for the NOx abatement data using stoichiometric conversion reactor models to approximate the chemistry involved. We show that the model is capable of accurately simulating the base-case data. At this point, we have simply calculated a mass balance and hypothesized the

predominant reaction pathways. We note and explain the discrepancies between our findings and the material balance provided by personnel at RFAAP.

When we attempt to extend the model to various design and process variables adjustments through sensitivity tests, the model is found lacking. It cannot represent the behavior shown in the experimental literature for similar processes. Thus, more work needs to be done on the model and aspects of the reaction chemistry used. Though the chemistry utilized in the model represents a "stoichiometrically accurate" approximation (it can fit the base-case mass balance), it fails mechanistically and does not follow true system behavior in response to manipulated variables.

3.1.2 Introduction to NOx Removal at RFAAP

The literature review in Chapter 2 concerns itself primarily with an overview of the most utilized NOx removal technology and a brief introduction to absorption coupled with SCR. The remainder of this document focuses on the process located at the Radford Facility and Army Ammunition Plant (RFAAP) in Radford Virginia. We hope applications from this thesis can be extended to similar processes in operation, in construction, and in the design stages at other sites. The process at RFAAP makes use of absorption/SCR technology as discussed in Section 2.4.

In the sections on computer model development, we state all assumptions and address their consequences on the generalization of results and conclusions to similar

processes. Conclusions referring to simulation results apply to the range of operating conditions explored here. Similar processes under different conditions can make certain of our assumptions invalid for those processes in question. The complexity of NOx chemistry and processing makes proper selection of assumptions and operating conditions of utmost importance.

3.1.3 Purpose of NOx Abatement at RFAAP

The nitrocellulose plant at RFAAP uses highly concentrated nitric and sulfuric acid to nitrate cotton linters to produce nitrocellulose. The reaction is run at atmospheric pressure in large stainless steel vats (atmospheric pressure for the altitude of the Radford site is approximately 14.1 psia, 0.959 atm, 97.2 kPa). Concentrated nitric acid can vaporize and also decompose in water to form NOx gases in appreciable amounts. Sulfuric acid can do the same to a lesser extent. Without some form of treatment for these fumes, they escape to the atmosphere causing damage to the environment and subject RFAAP to fines levied by governmental agencies.

In 1993, RFAAP purchased and installed a NOx abatement system for removing nitrogen oxide (NOx) gases from fumes that originate from their nitrocellulose plant. The NOx abatement system performs flue-gas treatment essential to the compliance of the plant to new guidelines laid down by the Environmental Protection Agency's (EPA) Clean Air Act and further restrictions outlined by the Commonwealth of Virginia Department of Environmental Quality (DEQ). The emissions limits set aside for the

effluent fumes from the nitrocellulose line at RFAAP in the stationary source permit from DEQ are as follows: 125 ppmv (as an hourly average), 2.8 lbs/hr, or 12.3 tons/yr for NOx. Sulfur dioxide limits are as follows: 92 ppmv (as an hourly average), 4.0 lbs/hr, or 17.5 tons/yr.

The recent performance of the SCR has not been satisfactory. Considering its intermittent shutdown, tightening environmental regulations, and the possibility of optimization and retrofit options, we choose the NOx abatement system and all associated equipment for ASPEN Plus computer simulation and modeling.

3.1.4 Process Description

In brief, the process receives NOx-rich fumes (NOx, in this case, consists of mostly NO_2 and NO with other NOx compounds formed from the dimerization of these two molecules, with NO_2 making up the bulk) from the nitrocellulose production line on site. As alluded to in Chapter 2, the situation where NO and NO_2 are mixed in the vapor provides the engineer with unique challenges, as well as opportunities for treatment. In general, removing NO and NO_2 require different processes to be successful. RFAAP utilizes absorption to remove NO_2 and SCR to remove NO.

A scrubber/absorber section absorbs some of the NOx gases and converts a portion to nitric acid. The remaining NOx fumes proceed to a catalyst vessel that uses ammonia (fed by steam vaporization) to reduce the NOx to atmospheric nitrogen, N_2.

The gases proceed from the catalyst vessel to the stack and out to the atmosphere. Figure 3.1 shows the simplified NOx abatement process.

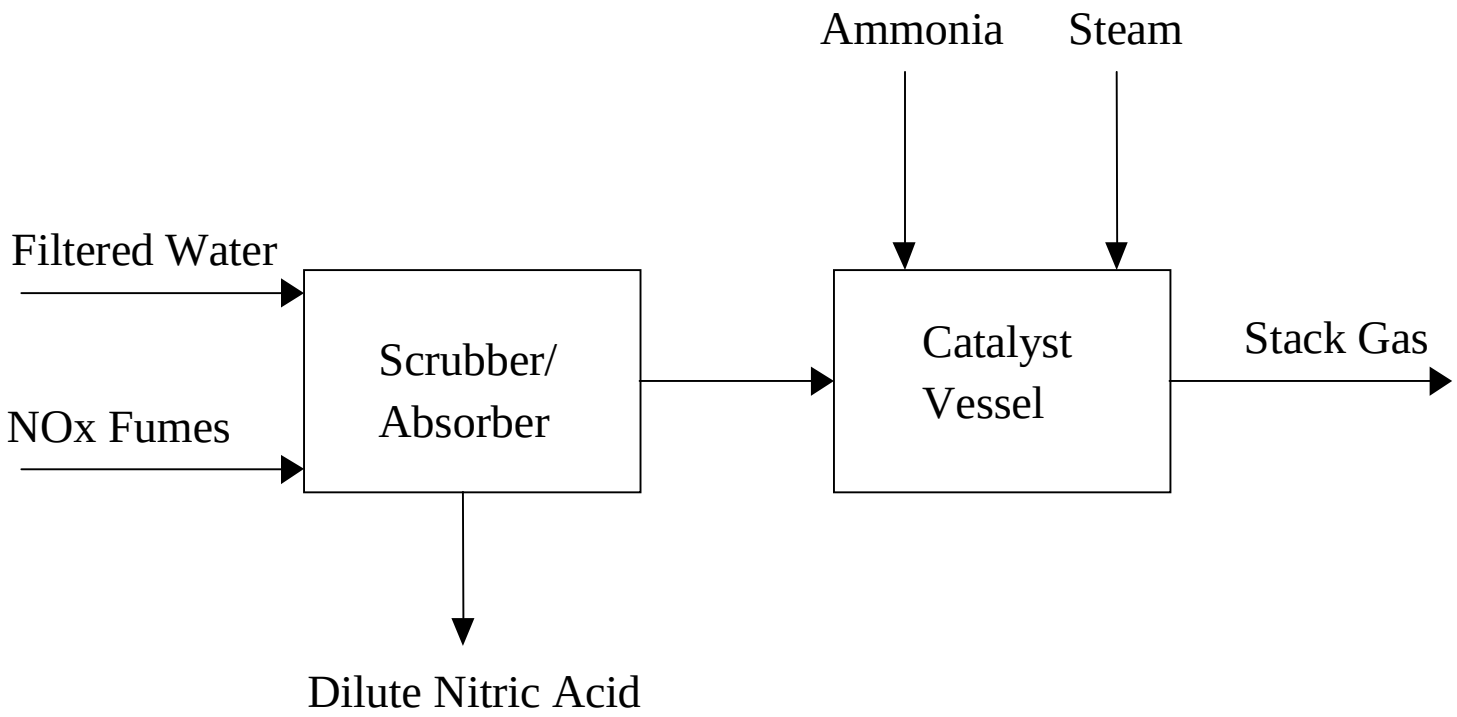

Figure 3.1. Simplified design of the NOx abatement process flow diagram.

We show a highly simplified block flow diagram for NOx abatement in Figure 3.1. This figure clearly shows the two main sections of the process. The scrubber/absorber mainly removes NO_2 and its derivatives (actually producing a limited amount of NO), whereas the catalyst vessel mainly removes NO. The two sections perform different tasks in the reduction of NOx and also work relatively independently of each other. We will treat them as such in the computer simulation discussion.

A scrubber/absorber unit, a stream preheater, a feed/effluent heat exchanger, a direct-fired natural gas heater, and a catalyst vessel reactor make up the main components of the process. These units can be seen in the more detailed block flow diagram represented in Figure 3.2. Fumes from the nitrocellulose (NC) line (greater than 97% air by volume with the remainder being NOx gases) feed into the bottom of the scrubber/absorber. Filtered water feeds to the top of the scrubber/absorber. The scrubber/absorber forces contact between the fumes and the water in order to absorb as much of the NOx gases as possible into the aqueous phase. Absorbed NOx compounds react with water to form nitric acid. The absorbing section separates the dilute nitric acid from the NOx gases. Dilute nitric acid leaves the bottom of the scrubber for waste-acid treatment or recovery.

The remaining NOx gases leave the top of the absorber for further treatment by selective catalytic reduction (SCR). A demister removes any entrained water vapor and nitric acid. A preheater in the line heats the NOx gases with steam. A feed/effluent heat exchanger further heats the NOx gases using the outlet from the catalyst vessel as the hot

stream. From there, a direct-fired heater uses natural gas combustion to heat the NOx gases to the required reaction temperature.

Ammonia feeds just ahead of the catalyst vessel, mixing with the NOx fumes. Automated control of the ammonia feed ensures proper reaction stoichiometry to minimize *the ammonia slip*, that is, unreacted ammonia that leaves the catalyst vessel in the effluent, and to maximize the amount of NOx reduced. Steam also feeds to the catalyst vessel, serving to diffuse and vaporize the ammonia in a safe manner. The catalyst promotes several simultaneous reactions, which will be discussed in detail later, that reduce the NOx gases to N_2 (atmospheric nitrogen) and H_2O with ammonia as the reducing agent. The outlet stream of the catalyst vessel preheats the NOx gas in the aforementioned feed/effluent heat exchanger. The catalyst-vessel effluent passes through the feed/effluent heat exchanger on its way to the vent stack. Figure 3.2 shows the arrangement of equipment and streamlines in the NOx abatement system.

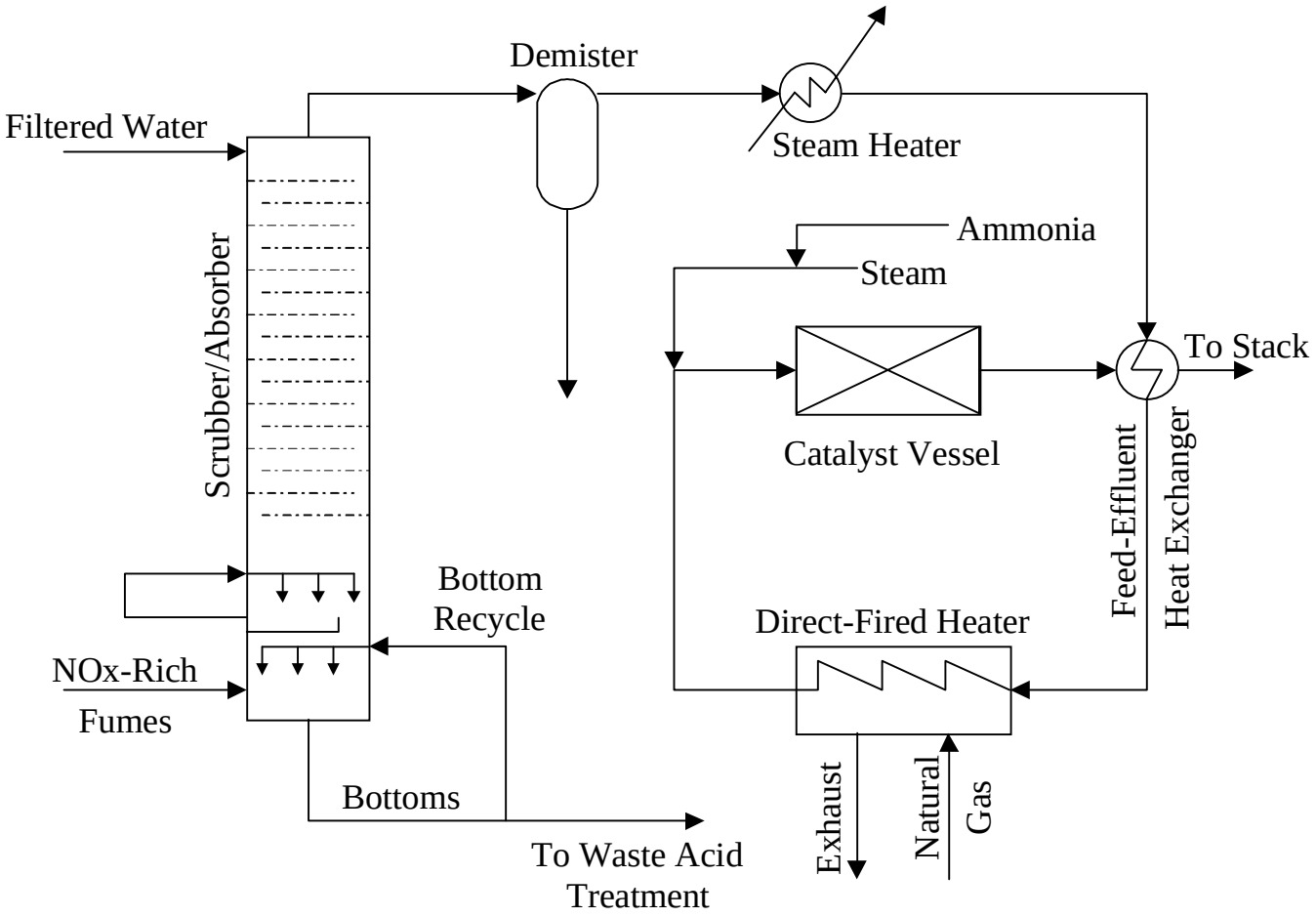

Figure 3.2. Block flow diagram of NOx abatement system provided by RFAAP.

3.2 Detailed Explanation of Process Equipment

3.2.1 Scrubber/Absorber

The scrubber/absorber is the first major unit in the NOx abatement system. The introduction briefly outlined the purpose of this unit. A more detailed examination follows. The column consists of two sections: The top of the column is the staged absorber section, and the bottom is a two-stage scrubber tank with its familiar spray nozzles. Fumes composed of air rich in NOx gases from the nitrocellulose line of RFAAP feed into the bottom of the scrubber section, while filtered water feeds into the top of the absorber section. Filtered water covers the absorber stages and flows down the downcomers. The staged absorber section consists of 16 bubble-cap trays. Each tray has 79 equally spaced bubble-caps. Figure 3.3 details the upper portion of the scrubber/absorber column. We number the absorption section bubble-cap trays from the top down as per the ASPEN convention. Figure 3.4 shows the tray arrangement. Figure 3.5 gives an expanded view of a bubble cap and downcomer area of a tray.

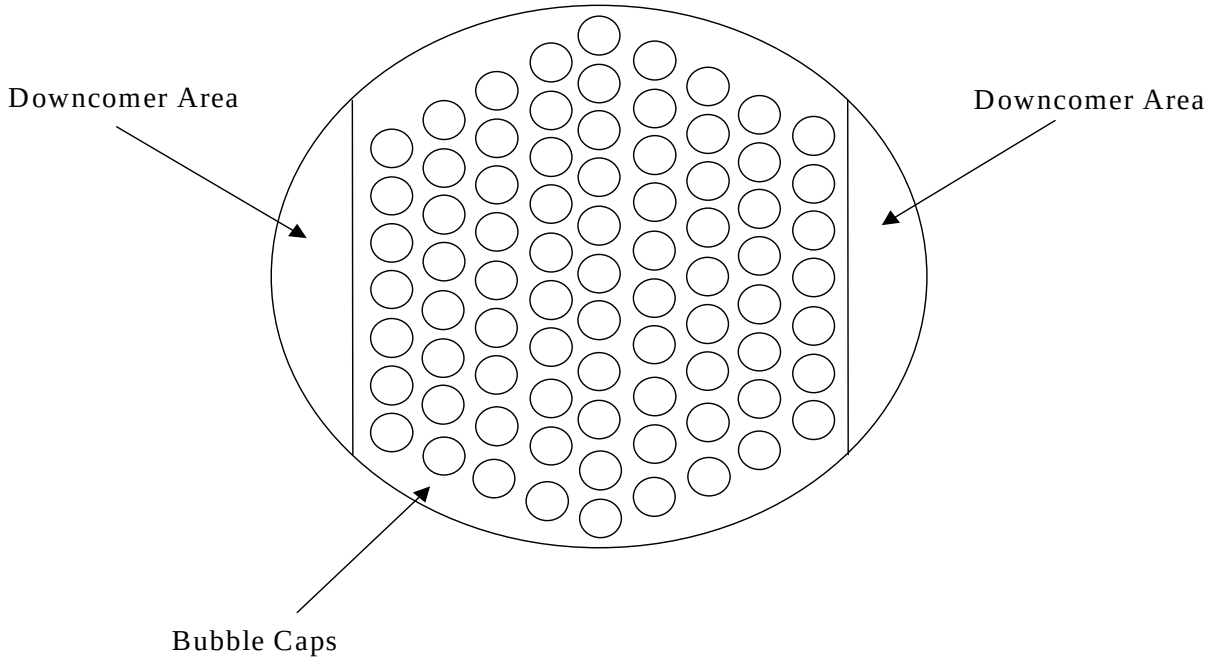

Figure 3.3. Schematic of bubble-cap tray arrangement.

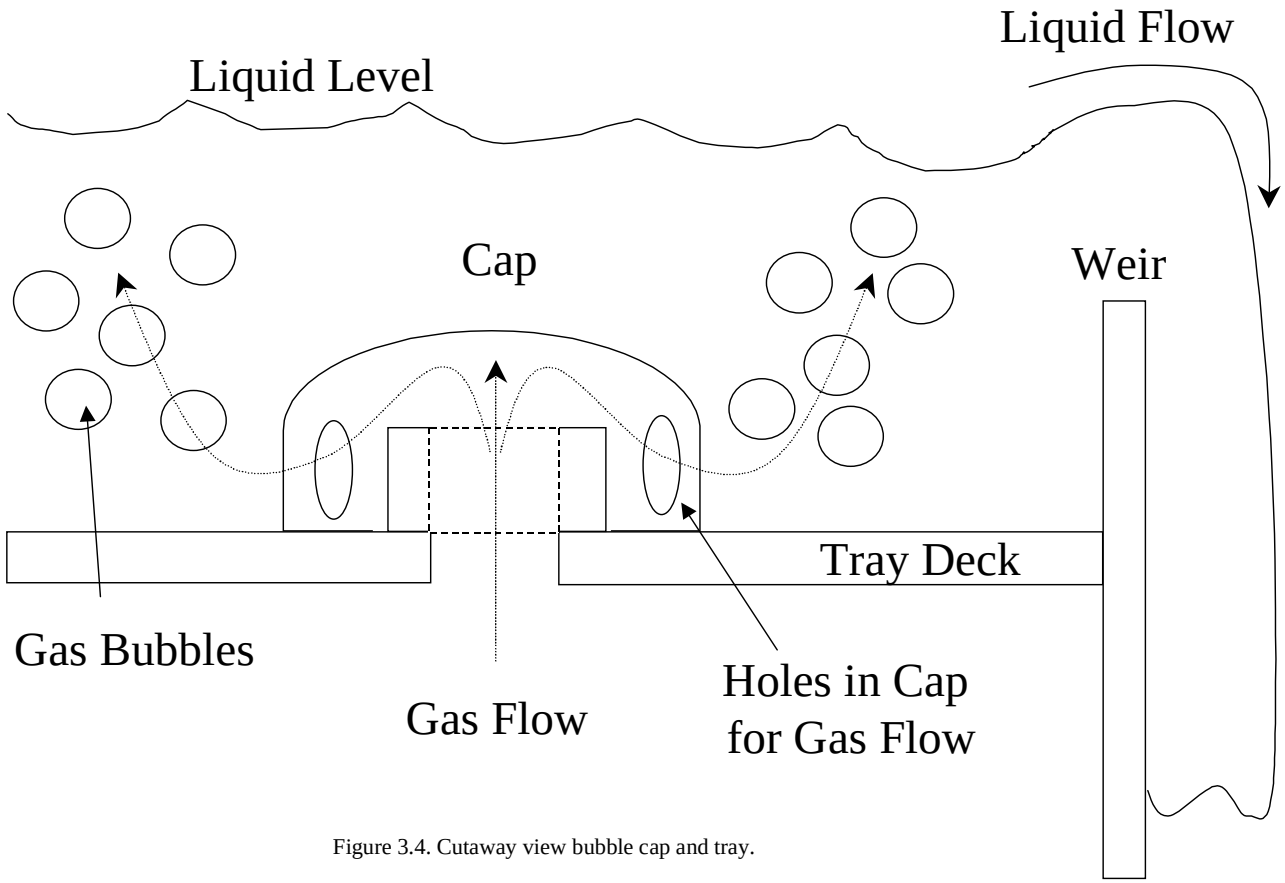

Figure 3.4. Cutaway view bubble cap and tray.

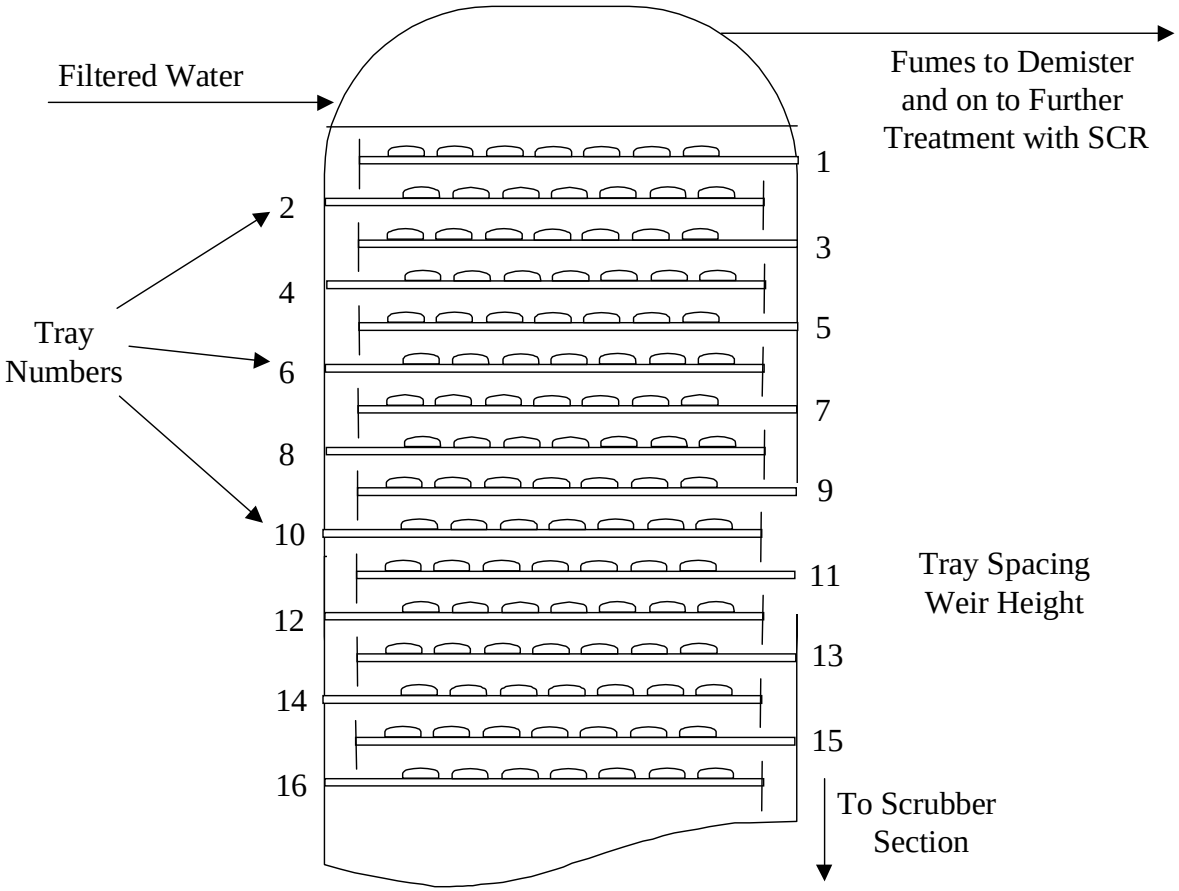

Figure 3.5. Detailed schematic of absorption section of scrubber/absorber tower.

The scrubber section begins below the bottom tray of the absorber. Figure 3.6 details the scrubber section of the scrubber/absorber tower. The scrubber section consists of two spray nozzle stages. Figure 3.7 shows the design of the spray nozzles within the scrubber section of the column. A catch basin collects the water and funnels it to a recycle line. A pump in that line pumps the water up to a spray-nozzle section just below the bottom absorber tray. Water that overflows this catch basin goes to the bottom of the column where it is drained. Pumps send it to a splitter where some is recycled back to a second spray nozzle below the first nozzle. The remainder leaves as a waste-acid stream. A vent-gas fan blows the fumes from the NC line to the bottom of the column. The fumes contact the sprayed water in the scrubber section and bubble up through the absorber trays. Some of the NOx gases are absorbed into the aqueous phase.

Reactions, which produce nitric acid from the NOx gases, occur throughout the scrubber/absorber. Table 3.1 shows the reactions that occur in the scrubber/absorber as proposed by personnel at RFAAP. In Chapter 4, we will show that this set of reactions, though accurate as far as stoichiometry, is incomplete and misleading. However, correct stoichiometry is all that is needed for a conversion-reaction model. Thus, we will proceed.

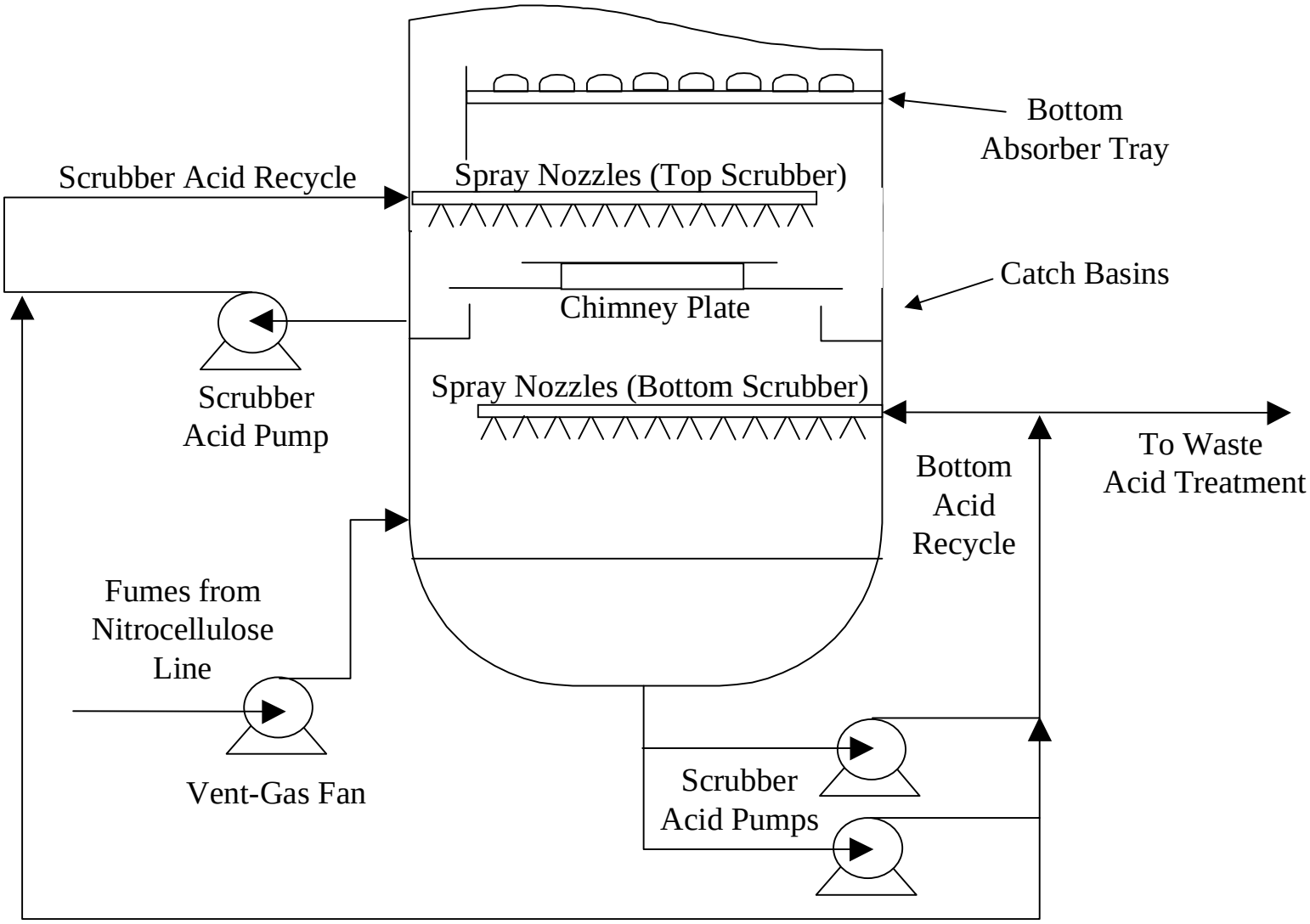

Figure 3.6. Cutaway view of the scrubber section of the scrubber/absorber tower.

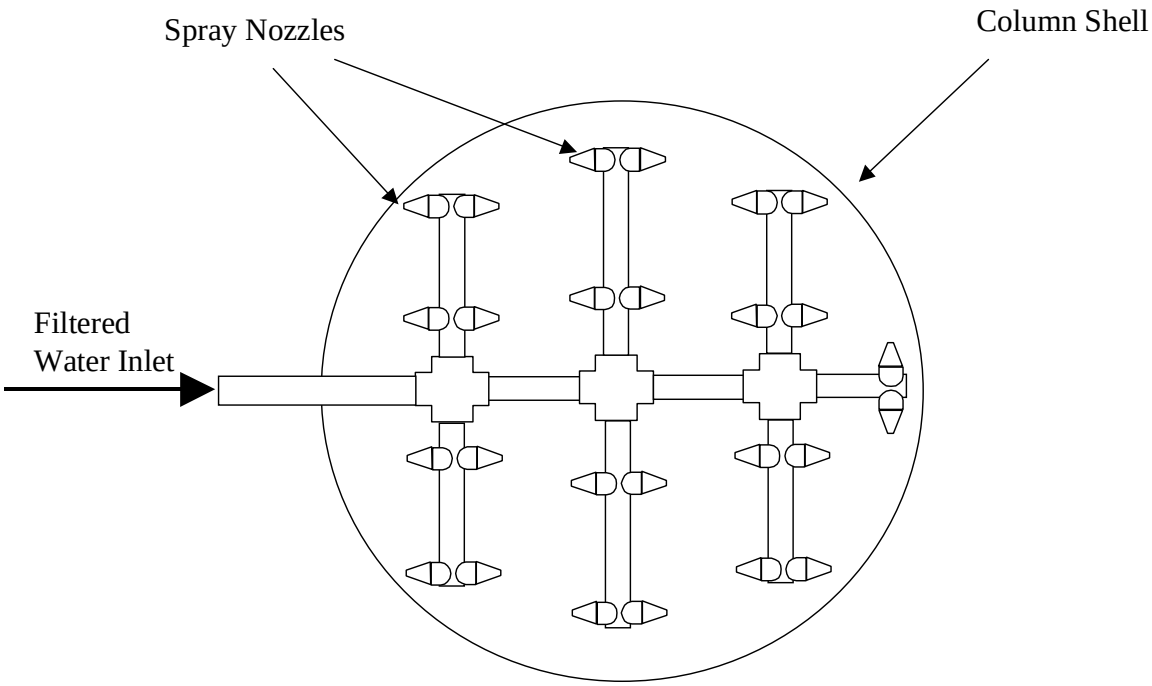

Figure 3.7. Detailed view of the spray nozzles used in the scrubber section of the scrubber/absorber tower.

Table 3.1. Reactions occurring in the scrubber/absorber as proposed by personnel at RFAAP.

Rxn. #	Reaction Stoichiometry
3.1	$2NO + O_2 \leftrightarrow 2NO_2$
3.2	$2NO_2 + H_2O \leftrightarrow HNO_3 + HNO_2$
3.3	$3HNO_2 \leftrightarrow HNO_3 + H_2O + 2NO$
3.4	$3NO_2 + H_2O \leftrightarrow 2HNO_3 + NO$

We see that reaction (3.4) results from the addition of reaction (3.3) and reaction (3.2) multiplied by a factor of three. Additionally, nitric acid (HNO_3) dissociates in aqueous solution in an ionization reaction. Table 3.2 shows this reaction. Nitric acid is a strong acid that quickly and almost completely dissociates in solution. Therefore, ionization consumes HNO_3 almost as quickly as it is produced. This tendency drives the equilibrium of the above reactions to the products. Table 3.1 shows that the net result of these reactions is the conversion of NO to NO_2, and the subsequent conversion of NO_2 to HNO_3 (nitric acid). Nitric acid then dissociates, yielding a proton (H_3O^+ is a more realistic representation for than H^+) and a nitrate ion as per reaction (3.5) in Table 3.2. Figure 3.8 gives a visual representation of the reaction network for NOx absorption.

Table 3.2. Dissociation reaction of nitric acid in aqueous solution.

Rxn. #	Reaction Stoichiometry
3.5	$HNO_3 + H_2O \leftrightarrow H_3O^+ + NO_3^-$

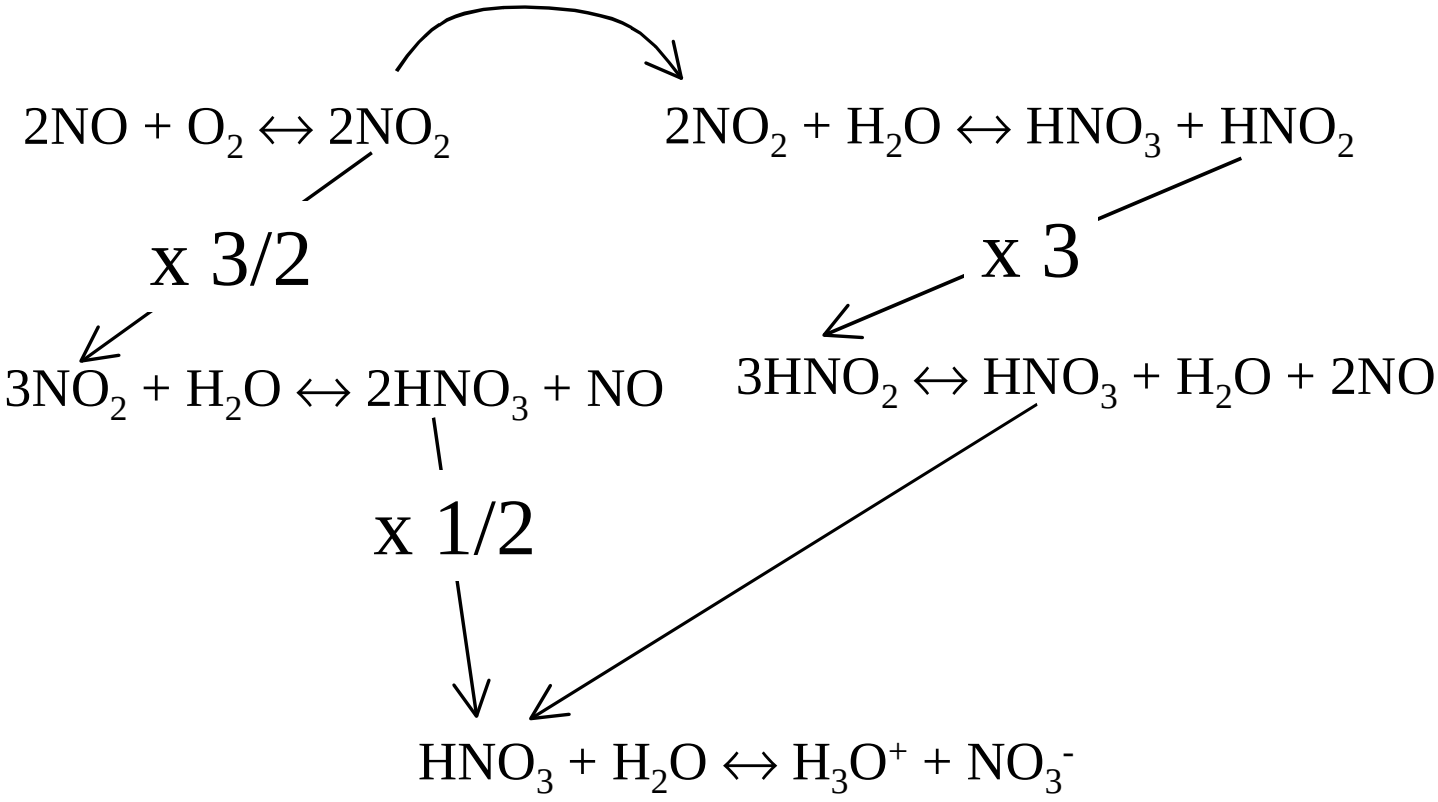

Figure 3.8. Visual representation of reaction network proposed by RFAAP.

This reaction set is not a pure chain reaction because a mixture of NO and NO_2 are fed to the system. If NO was the main component of the NOx, as is the case in most combustion processes, then reaction (3.1) would represent the rate-limiting reaction for this sequence.

These reactions accomplish the dual goals of eliminating the source of NOx emissions, as well as producing nitric acid (HNO_3). Nitric acid, a compound that absorbs into the aqueous phase readily and, after dissociation, has a strong tendency to stay there, also represents a potentially valued product. In high enough concentrations, the nitric acid can be recovered, not only adding to the product yield, but also eliminating the cost required for wastewater treatment from this process.

Given a large enough residence time, the strong equilibrium tendency to products for this reaction set facilitates pollutant removal. The production of the nonvolatile nitrate ion (NO_3^-) and the insoluble NO as the final products of the reaction network constitute the major driving forces for NO_2 absorption. The nitric acid leaving the scrubber/absorber is dilute and of a small quantity. It does not contribute greatly to the wastewater duties of the plant. We will discuss the possibility of its recovery in later sections. Recall that aside from the obvious nitric acid dissociation reaction, RFAAP proposed this reaction network. Though we contend that it is incomplete as a mechanism, the overall stoichiometry is correct, and we will attempt to model the process using it. The reader should note that no distinction has been made for the reactions or the

components themselves as to which phase they take place or predominate. We will show in this and the following chapters that this reaction heterogeneity becomes a major problem for proper simulation. Thus, the eventual failure of the conversion model will become the impetus for the subsequent equilibrium and kinetic models.

3.2.2 Demister

The demister, installed on the outlet of the top of the absorber column, consists of a simple tank packed with wire-mesh screens. Entrained liquid impacts with the screening and trickles to the bottom of the demister where it flows down to a drain that leaves the wastewater treatment area of RFAAP. Figure 3.9 shows a simple schematic diagram of the demister. No data are available from RFAAP on the composition or flow rate of the liquid flow from the bottom of the demister aside from the fact that it constitutes a "trickle." Also, coming from the top stage of the absorber, this stream should contain very little NOx or nitric acid. We have therefore assumed it to be negligible.

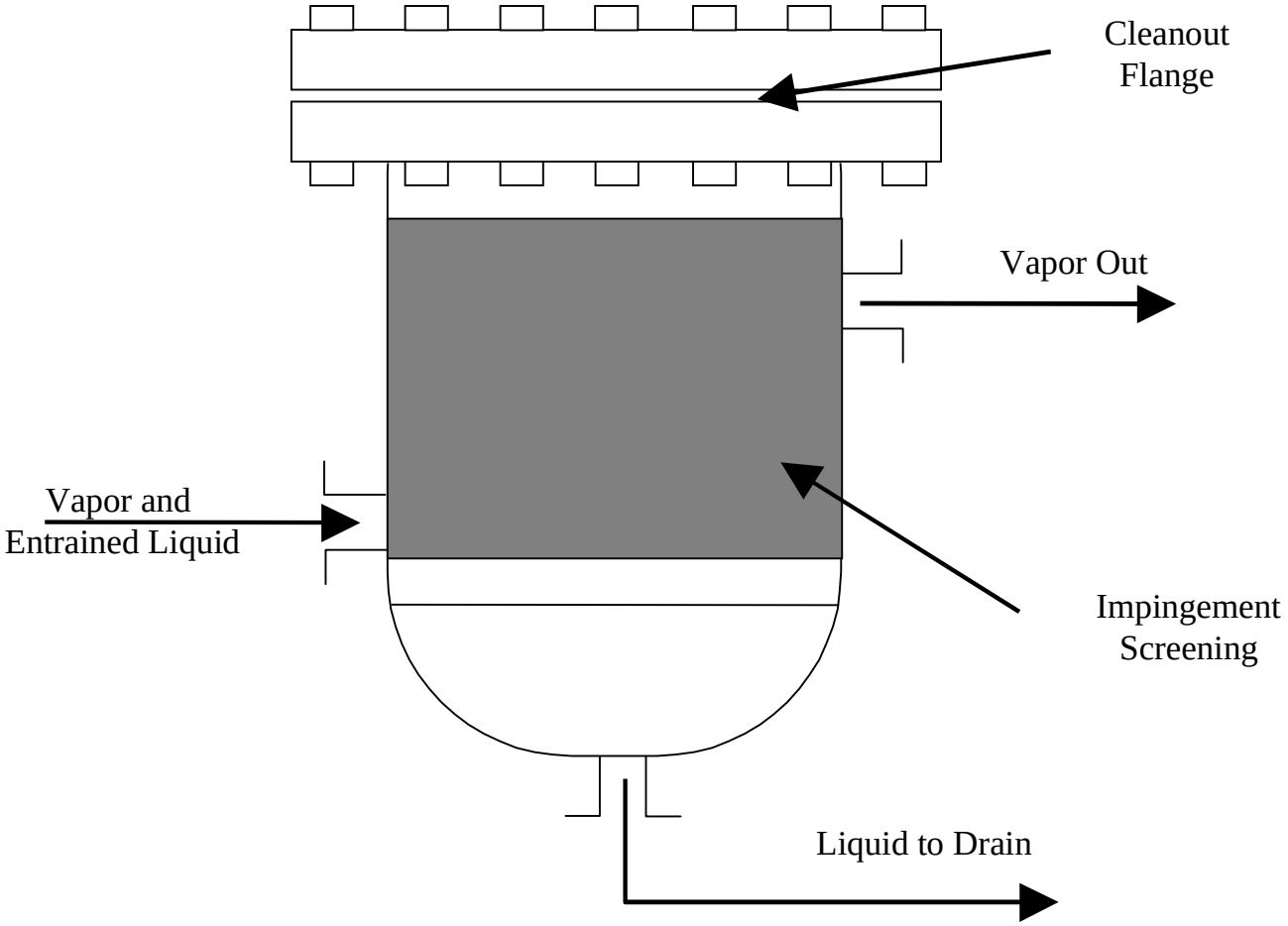

Figure 3.9. Detailed diagram of demister construction.

3.2.3 Heat Exchangers and Process Heaters

The fumes leave the absorber at nearly ambient (approximately 80 ^{o}F, 27 ^{o}C) temperature. For selective catalytic reduction with ammonia, the temperature of the fumes must be raised to approximately 600 ^{o}F (316 ^{o}C), thus requiring a temperature rise of at least 520 ^{o}F (289 ^{o}C) for a flow rate of approximately 18,600 lb/hr (4000 scfm) consisting mostly of air. Table 3.3 lists the different temperature-change operations in the NOx abatement system, including the flowsheet connectivity and inlet/outlet temperatures.

Table 3.3. Process streams, heating units and the temperature changes affected.

Equipment Name	Stream In From:	Stream Out To:	Inlet Temp., ^{o}F (^{o}C)	Outlet Temp., ^{o}F (^{o}C)
Preheater	Demister	Economizer	80 (27)	100 (38)
Economizer	Preheater	Direct-Fired Heater	100 (38)	406 (208)
Economizer	Catalyst vessel	Stack	650 (343)	350 (177)
Direct-Fired Heater	Economizer	Catalyst Vessel	357 (181)	600 (316)

Notes: values are those provided by Radford

The preheater uses utility steam to raise the fume temperature from 80 ^{o}F (27 ^{o}C) to 100 ^{o}F (38 ^{o}C). After the preheater, the countercurrent economizer (also known as the feed/effluent heat exchanger) uses the effluent from the catalyst vessel to raise the fume temperature to 406 ^{o}F (208 ^{o}C). The direct-fired heater combusts natural gas within the shell, while the fumes flow through a U-tube in the heat exchanger. Within this unit, the fume temperature rises to approximately 600 ^{o}F (316 ^{o}C). Selective catalytic reduction is highly exothermic so the fume temperature rises within the catalyst vessel, from 600 ^{o}F (316 ^{o}C) to 650 ^{o}F (343 ^{o}C). Figures 3.10, 3.11, and 3.12 show the steam preheater, feed/effluent heat exchanger, and direct-fired heater respectively.

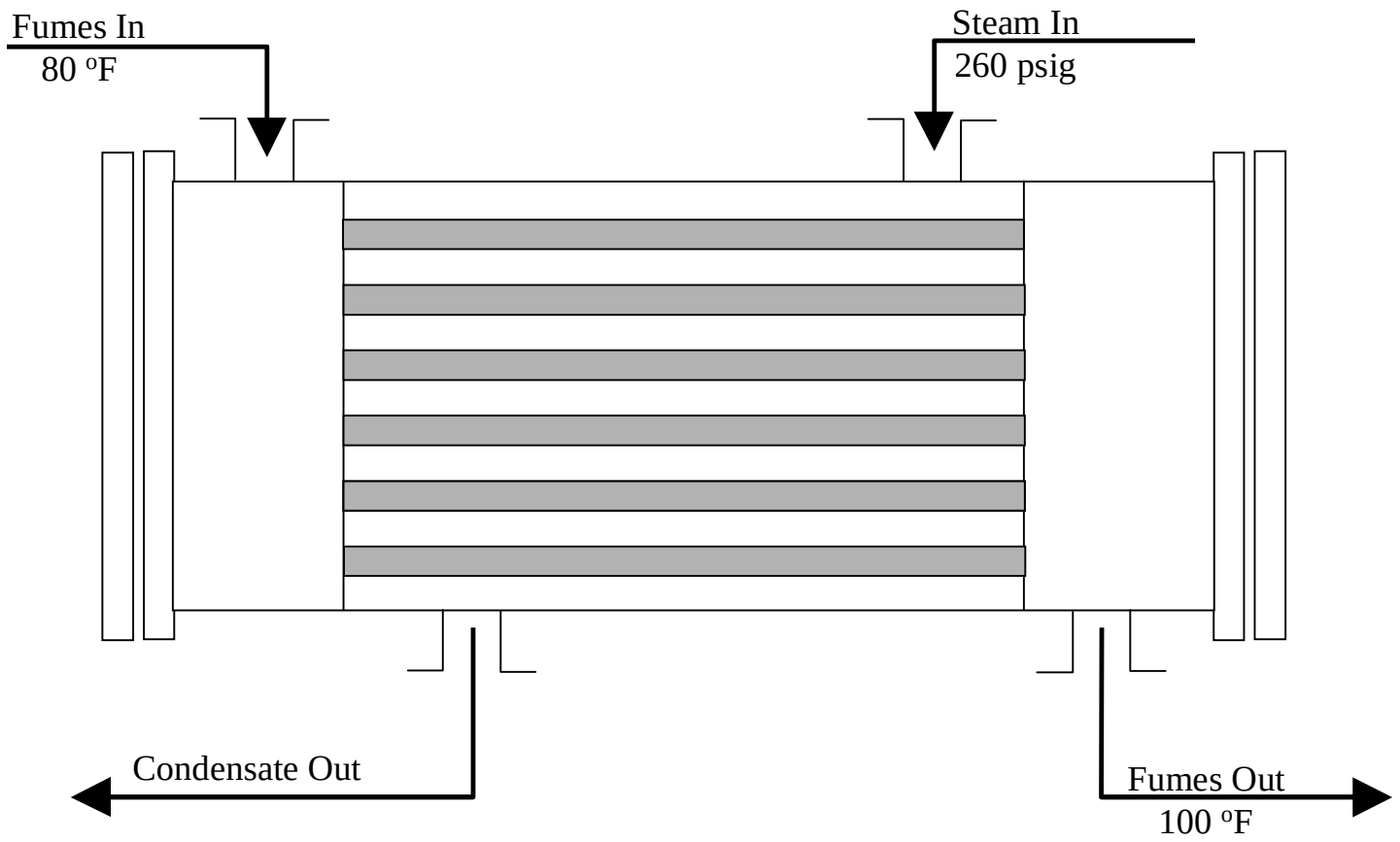

Figure 3.10. Detailed diagram of steam preheater.

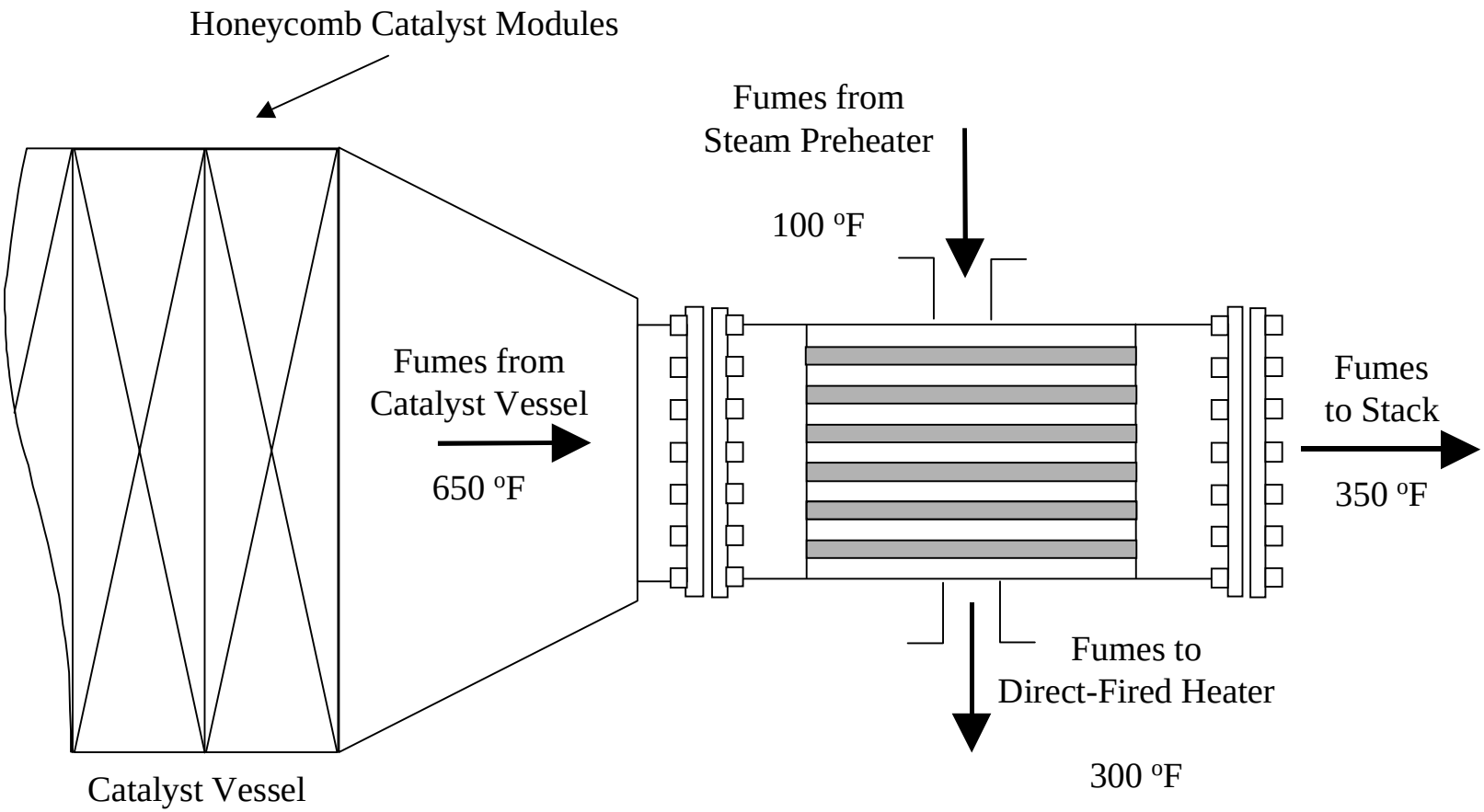

Figure 3.11. Detailed diagram of feed/effluent heat exchanger (economizer).

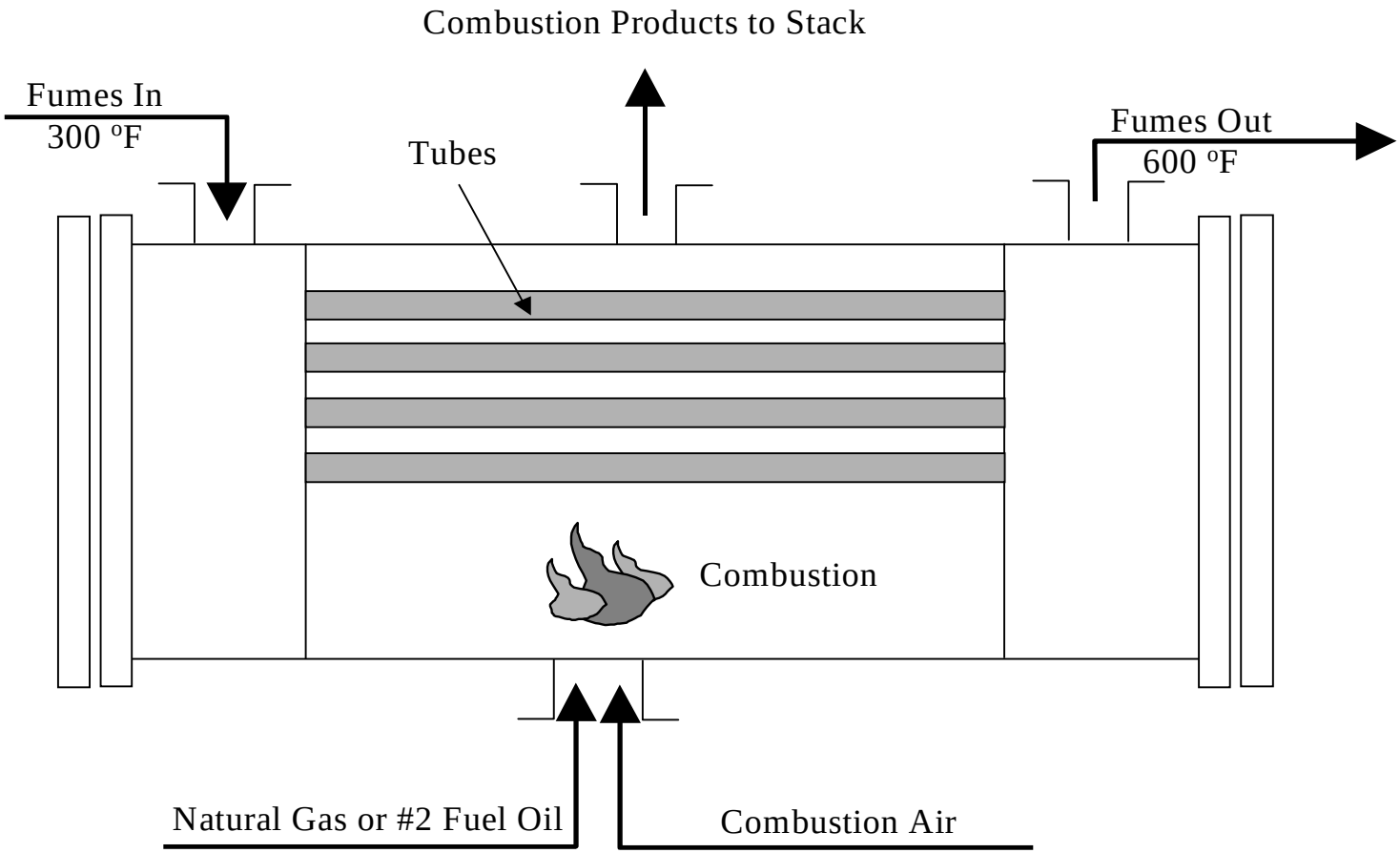

Figure 3.12. Detailed diagram of direct-fired heater.

3.2.4 Catalyst Vessel

Ammonia and steam mix with the NOx gases downstream of the direct-fired heater. This mixture feeds into the catalyst vessel. Ammonia reduces the NOx gases over a vanadia-supported-on-titania (V_2O_5 on TiO_2) catalyst bed. Catalyst blend recipes are highly proprietary and we were not given exact details on the makeup of the catalyst. We know that it consists of less than 5% vanadia on less than 85% titania (both weight percentages). Reaction rate and selectivity depends heavily upon catalyst blend recipe. However, the mass balance provides a good starting point. Table 3.4 shows the reactions that are thought to occur in the catalyst vessel.

Table 3.4. Reactions proposed for the catalyst vessel.

Rxn. #	Reaction Stoichiometry
3.6	$4NH_3 + 6NO \leftrightarrow 5N_2 + 6H_2O$
3.7	$4NH_3 + 4NO + O_2 \leftrightarrow 4N_2 + 6H_2O$
3.8	$2NO_2 + 4NH_3 + O_2 \leftrightarrow 3N_2 + 6H_2O$
3.9	$NO + NO_2 + 2NH_3 \leftrightarrow 2N_2 + 3H_2O$

Note: These reactions are provided by RFAAP

We see that the net effect of the selective catalytic reduction reaction is to consume NH_3 and NOx gases, while producing water and atmospheric nitrogen. We do not know which reactions predominate. However, at the point of input into the catalyst vessel, NO represents the preponderance of the NOx.

The catalyst vessel itself consists of stainless steel construction roughly in a three-dimensional rectangular prism configuration. Within this large rectangular prism are smaller boxes, called modules, that house the honeycomb catalyst bundles, called elements. These honeycomb catalyst elements, consist of support and active catalyst materials in a single piece. Hollow rectangular holes, called cells, run the length of the element and provide for high gas flow rates, as well as a large surface-area-to-volume ratio. Each element has a 20-by-20 cell arrangement for 400 total cells per element (cell number depends on application). Figure 3.13 illustrates a catalyst element used at RFAAP.

As they consist of fragile perforated ceramic, catalyst elements require a steel superstructure for transport and installation to reduce the chance of breakage. Many elements are bundled together within this steel structure to make up a module. We refer to the steel superstructure around the bundle of elements as the frame. The surface of the frame also interlocks with other framed modules acting as a gasket to seal the gas flow upon installation. Figure 3.14 shows a typical frame for a horizontal gas-flow application (similar to that used at RFAAP). Figure 3.15 gives a detailed view of the arrangement of the catalyst elements within the catalyst-module frame. Figure 3.16 shows the arrangement of the modules. The catalyst vessel at RFAAP runs at atmospheric pressure requiring only light construction. Figure 3.17 illustrates the construction of the selective catalytic reduction vessel which houses eight catalyst modules.

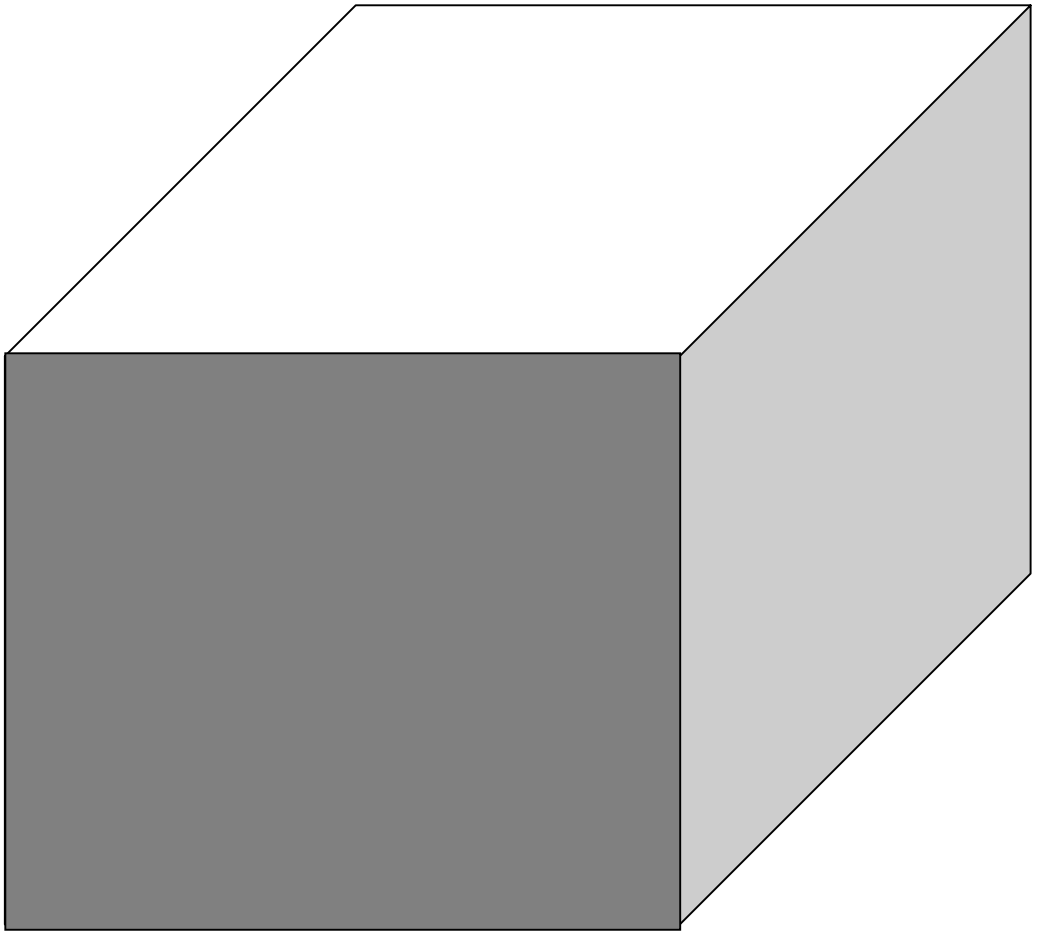

Figure 3.13. Detailed diagram of honeycomb catalyst element.

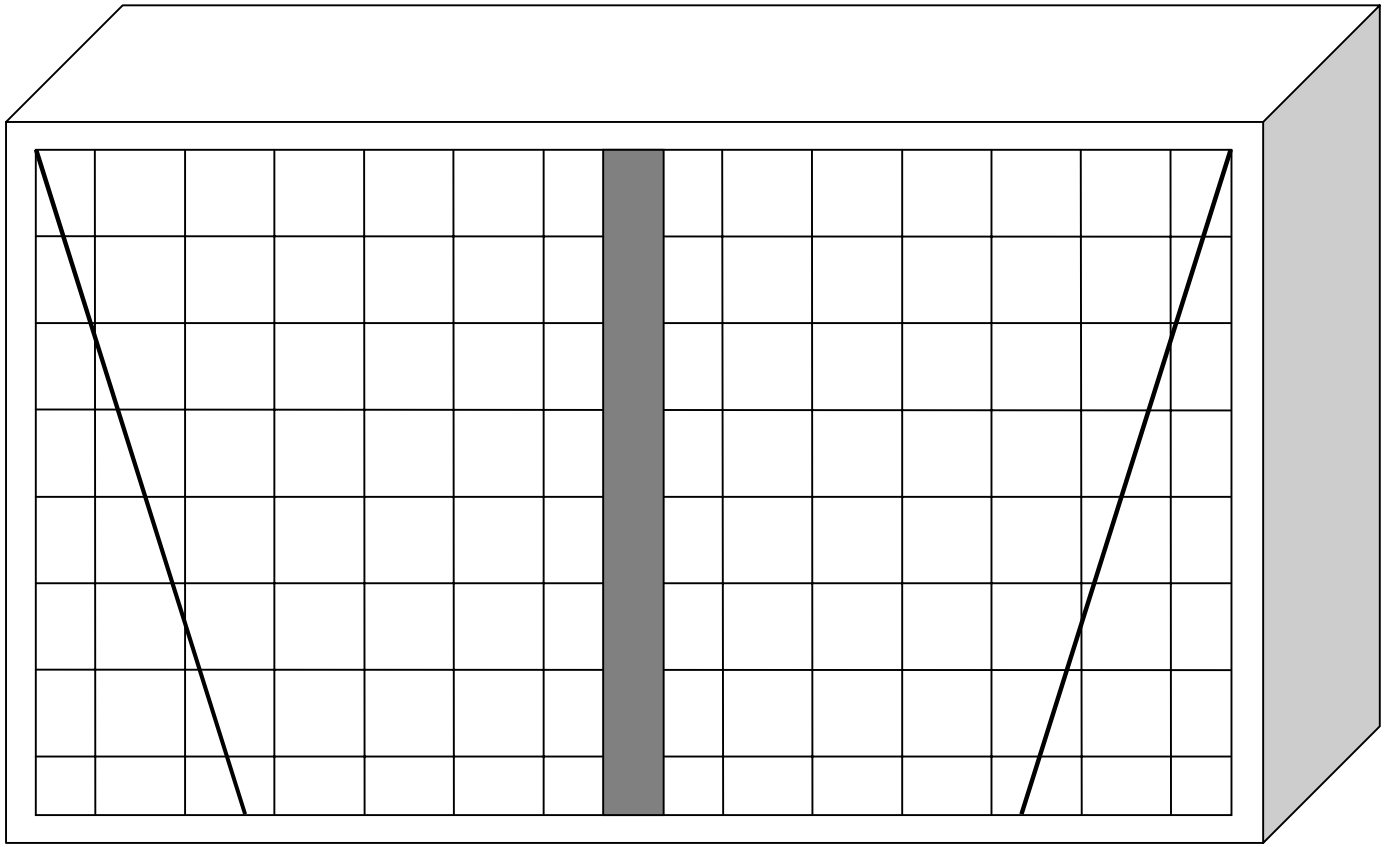

Figure 3.14. Catalyst module for horizontal flow, similar to those used by RFAAP.

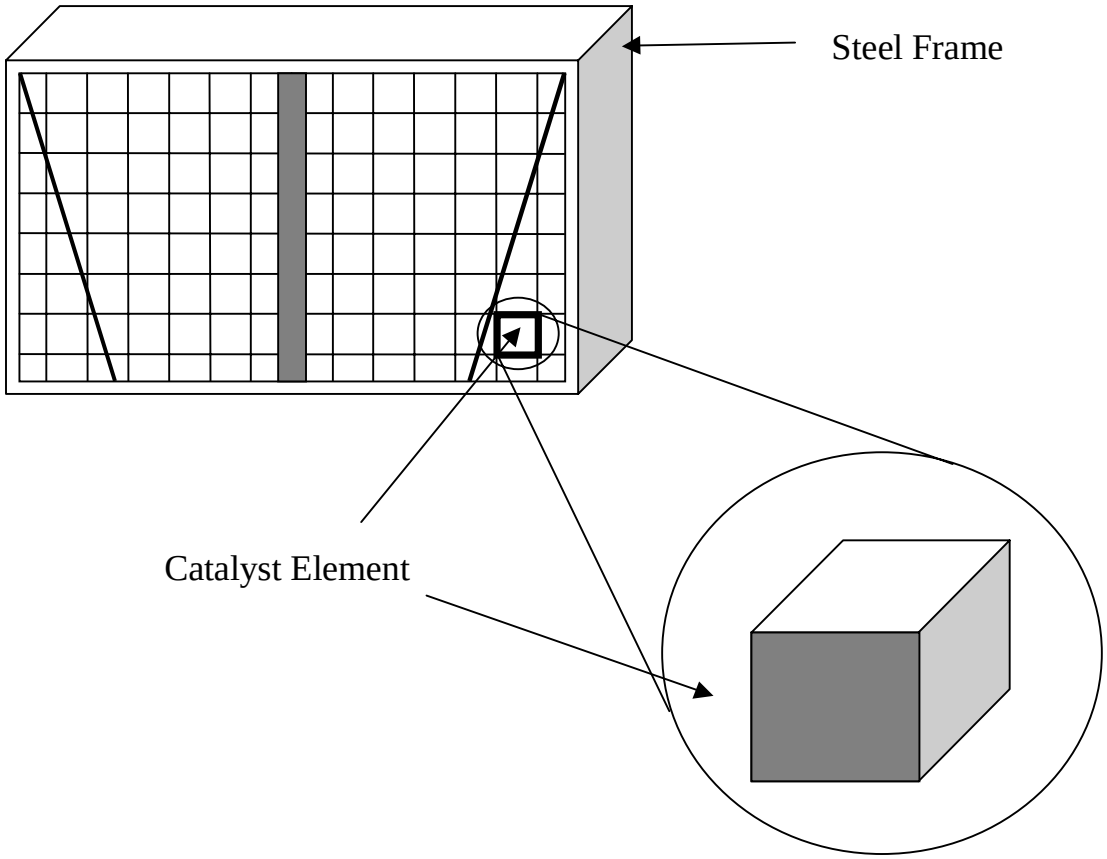

Figure 3.15. Detailed view of catalyst module with exploded view of catalyst element.

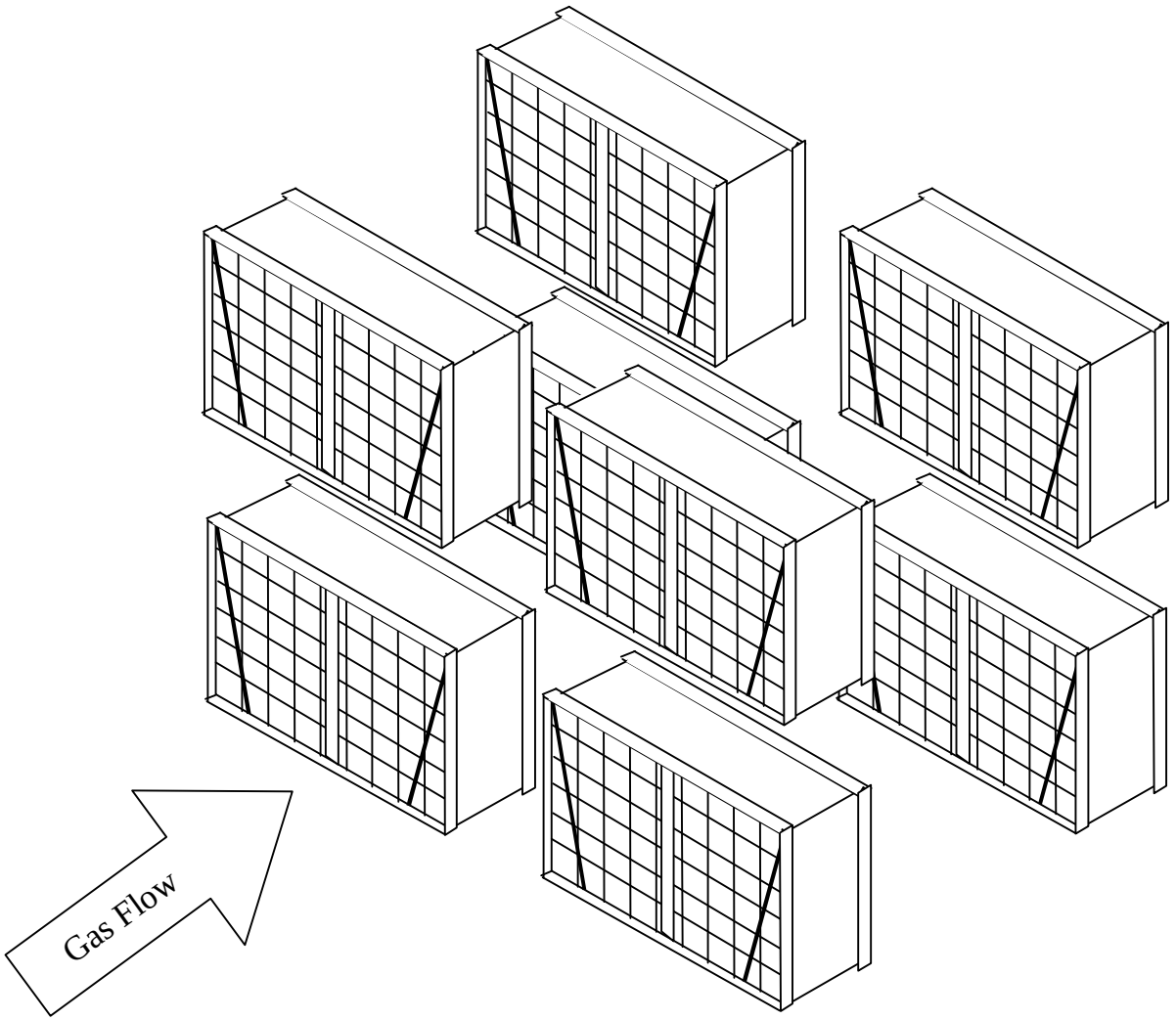

Figure 3.16. Catalylst module arrangement within the catalyst vessel.

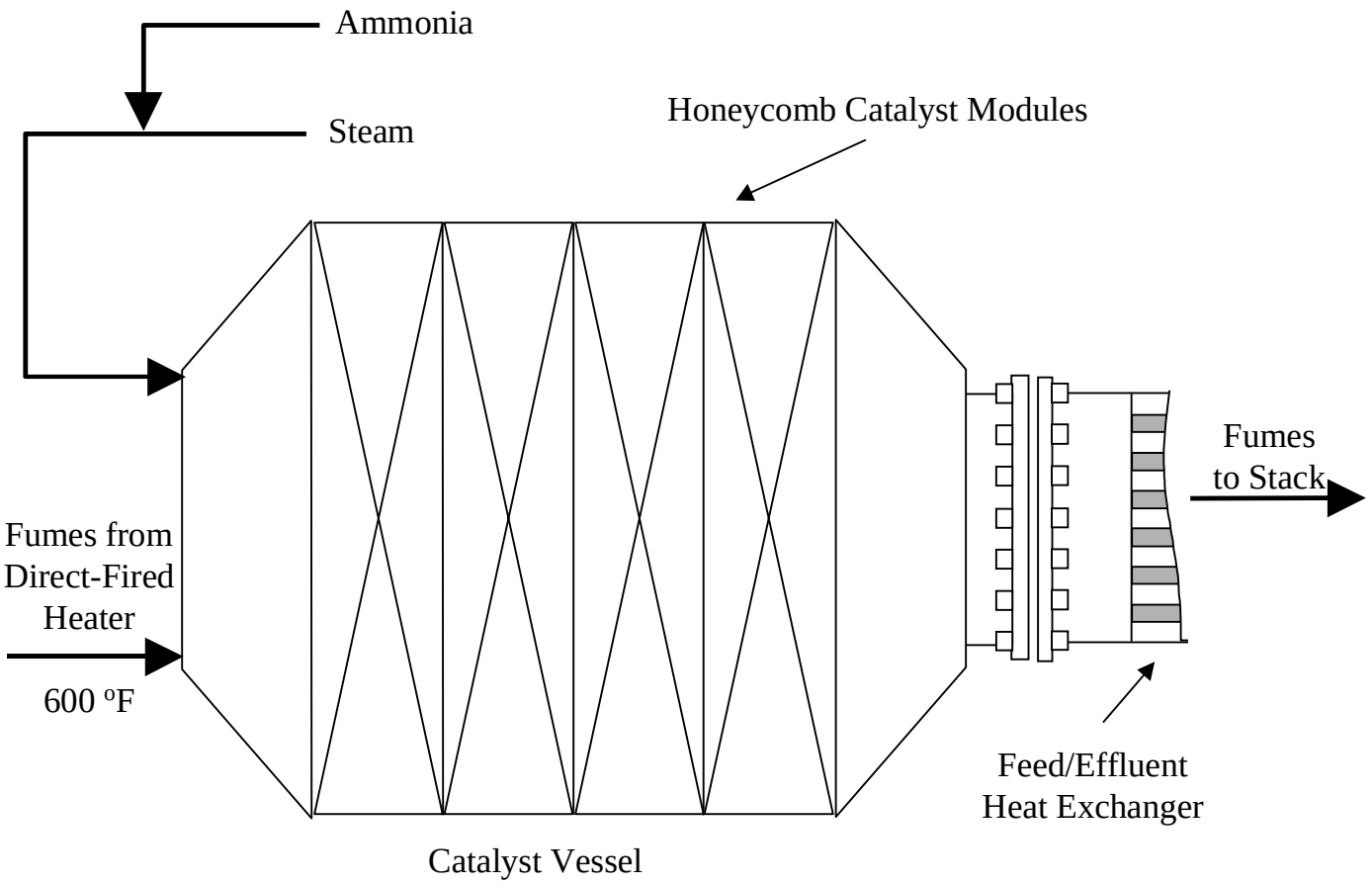

Figure 3.17. Diagram of catalyst vessel in relation to material streams and adjacent equipment.

3.2.5 NOx Abatement System Input and Output Flow Rates

Table 3.5 shows the input streams to the system as provided by RFAAP. Table 3.6 shows the output streams as provided by RFAAP. There are, however, more inputs and outputs than specified for us by RFAAP. In some cases, ASPEN helps us determine what those flows consist of. Other cases require us to make certain assumptions about the streams. Simple component mass balances fill in any holes left in the information. Table 3.7 shows the missing streams and their property values. The values have been calculated based on assumptions we make from information provided by RFAAP. The demister drain stream has been assumed to be negligible. RFAAP give the steam flow rate to the catalyst vessel as 21 lb/hr at 450 ^{o}F (232 ^{o}C). We assume 100% quality steam (all vapor) to arrive at the steam pressure of 422 psia (28.72 atm, 2910 kPa).

Table 3.5. Input flows to the system (values given by RFAAP).

Stream:	Fumes from NC Line	Filtered Water	Steam to SCR	Ammonia to SCR
Mole Flow lbmol/hr				
NO	0.39			
NO_2	3.37			
H_3N				1.37
O_2	132.2			
N_2	497.3			
H_2O	15.1	22.17	1.17	
H_2SO_4				
HNO_2				
HNO_3				
Total Flow lbmol/hr	648.34	22.2	1.17	1.37
Total Flow lb/hr	18601	399	21	23.3
Total Flow cuft/hr	75600	6.42	24.3	264
Temperature F	90	78	450	86
Pressure psi	20	44	422	30

Table 3.6. Output flows from the system (values given by RFAAP).

Stream:	To Waste Acid Treatment	Fumes to Stack
Mole Flow lbmol/hr		
NO		0.06
NO_2		Trace
H_3N		Trace
O_2		132.06
N_2		496.77
H_2O	13.1	23.86
H_2SO_4		
HNO_2		
HNO_3	2.1	
Total Flow lbmol/hr	20.8	654.75
Total Flow lb/hr	376	18631
Total Flow cuft/hr	0.094	4000
Temperature ^oF	86	350
Pressure psi	15.1	14.1

Table 3.7. Streams not specified by RFAAP (calculated or assumed).

Stream:	Steam to Catalyst Vessel	Demister Drainage
	Input	Output
Mole Flow lbmol/hr		
NO		
NO_2		
H_3N		
O_2		
N_2		
H_2O	1.17	
H_2SO_4		
HNO_2		
HNO_3		
Total Flow lbmol/hr	1.17	0
Total Flow lb/hr	21	0
Total Flow cuft/hr	24.3	0
Temperature ^oF	450	80
Pressure psi	422	14.1

3.3 Introduction to ASPEN Plus Simulation of NOx Abatement

3.3.1 Purpose for ASPEN Plus Simulation of NOx Abatement

The ideal mathematical/computer model is the simplest, most theoretically elegant model that accurately simulates the actual process in its base configuration. The model involves all the assumptions made about the process. First, the model must accurately reflect the base-case data for the actual process; this will be referred to as model accuracy. Next, it must account for results of process changes observed for the actual process; this will be referred to as model precision. We refer to a simulation as when the model is given inputs that are used to calculate outputs.

To determine the accuracy and precision of the model, we must give it known inputs and run it as a simulation, comparing the results to known outputs. Achieving this end requires a trial-and-error process that involves running the simulation, comparing the results to plant data, and making changes to the model to affect its accuracy. In this thesis, we will omit the details of how we arrive at each model in succession and focus on the results and conclusions drawn from the simulations of the final evolution of each model. Suffice it to say that much research and many simulations are run to arrive at the logic and science of each model.

In any case, the engineer must thoroughly research the process to know how the simulation should behave in response to process changes. The simulation must prove

itself to be accurate and precise before the engineer is justified in putting his/her faith in it. After the model consistently proves its accuracy and precision, the engineer can confidently approach previously unexplored process modifications, for which no previous data exist. Even then, the model must continuously prove its worth to retain the engineer's confidence in the simulation results.

Quite often, a good model makes apparent conclusions about the physical system that are not intuitively obvious. Filling in the holes in component mass and energy balances, as we discussed in the previous section for this case study, represents a good example of this ability of computer model simulations. We can use such conclusions as stepping stones to further optimization.

3.3.2 Motivation for a Conversion-Reaction Model

The majority of unit operations encountered by chemical engineers involve heat and mass transfer. It is often satisfactory to model these operations separately from simultaneous reactions. Equilibrium assumptions usually model heat- and mass-transfer processes quite accurately. Because most industrial reactions occur far from equilibrium, when dealing with reactions, engineers often use a constant-percentage conversion with respect to a key reactant to model a reactor.

The treatment of different processes separately often yields satisfactory results because time, space, and equipment boundaries usually keep the separate operations of

heat and mass transfer and reaction relatively isolated from each other. Also, because of the complexity of reaction engineering and the narrow range of acceptable operating parameters, process and design engineers usually do not wish to affect the performance of a working reactor. They may choose to achieve optimization in the preparation and separation processes, while leaving reactors alone. For optimization of most industrial reactors, the sheer complexity usually requires more research assets than are available to the typical process engineer.

The particular case of NOx abatement at RFAAP includes a heterogeneous catalytic reactor typical to many chemical plants. Here, we refer to the selective catalytic reduction catalyst vessel. As described above, we are limited in our options for improving the reactor performance because of the narrow range of performance for the catalyst as well as other constraints on the SCR that we will discuss later.

In addition to the familiar plug-flow reactor, the process being studied also includes a highly atypical absorption operation. In the scrubber/absorber, heat and mass transfer are intimately coupled with chemical reaction. In both obvious and subtle ways, temperatures, concentrations, and reaction rates and conversions affect each other. With the conversion model and computer simulation, we shall see if percentage conversions can accurately model the reactions in this operation under changes in process variables. Also, we will investigate system sensitivity to certain process variables. The reaction conversions will remain constant, but the thermal and vapor-liquid equilibrium will be

affected. We will compare the results to those found in the literature to determine the appropriateness of the conversion model over the relevant range of conditions.

3.3.3 ASPEN Simulation Procedure

Computer modeling and simulation represents a powerful technique for the process engineer. Equally useful for design and retrofit, the computer provides the process engineer with calculations for predicting equipment and process behavior. The speed at which information is available to the engineer by these techniques represents its real usefulness. This speed also provides the engineer with the ability to produce large quantities of erroneous data.

Computer simulations do not excuse the engineer from making critical assumptions and properly specifying the system, or of digesting the information that is produced. Modeling software is simply a black box that processes the engineer's input specifications and returns an output. Even with the proper input, the output still requires the proper interpretation. With these tools, the engineer's responsibility has not changed.

Perhaps the software itself poses the greatest challenge to the simulation engineer. Chemical process simulation software makes implicit and explicit assumptions within the unit-operation blocks that perform the calculations. The engineer must take these assumptions and their ramifications into account when extending simulation results to conclusions about the real process. Even with that caveat, computer simulation

represents a great improvement over attempts to apply literature studies to processes with different equipment and operating conditions.

3.3.4 The Conversion-Reaction Model

Due to the vast array of chemical processes available to the chemical industry, no single computer simulation block can accurately cover all possible equipment configurations. However, combinations of computer-generated processes can adequately model complex chemical behavior. The simulation engineer must configure the ASPEN model to accurately simulate the behavior of the real process. Key differences can be seen in the process as modeled by ASPEN when using stoichiometric conversion reactors to model the chemical reactions. Figure 3.18 shows the process as modeled in ASPEN for comparison.

The most readily apparent changes from the original process are the splitting of the scrubber/absorber into an absorption column and the addition of two scrubber tanks, as well as the addition of three stoichiometric reactors. Also, we add a flash unit below the bottom scrubber tank. Each stream and simulation block is designated with an eight-letter-maximum name. Figure 3.18, the detailed block flow diagram for the computer model, shows all the stream and block designations. Stream and block names appear in all capital letters.

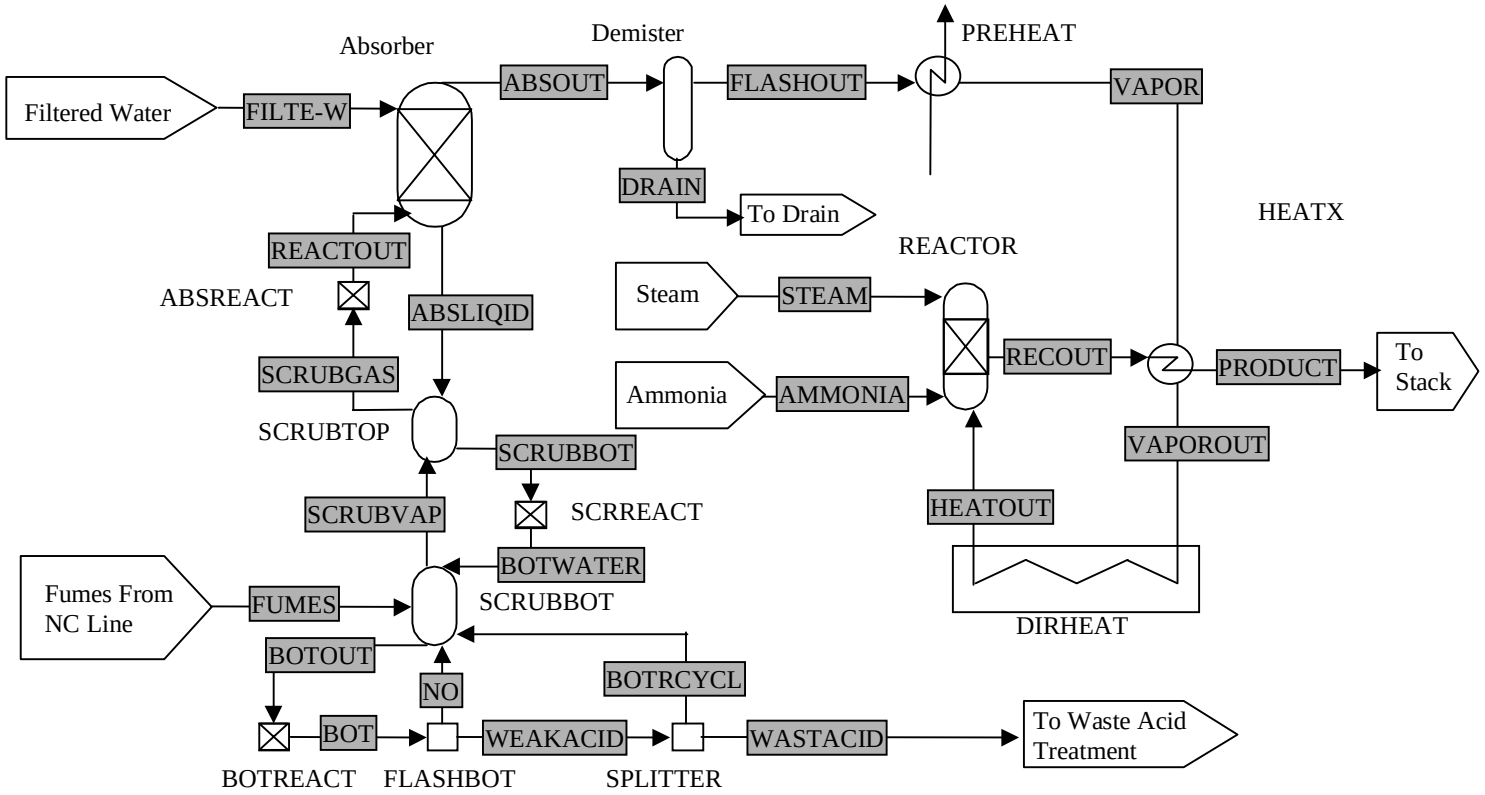

Figure 3.18. Flowsheet used for the conversion-model simulations.

The unit-operations modules available in ASPEN cannot accurately model certain real units that combine many chemical processes. As detailed earlier, the scrubber/absorber column performs the tasks of a scrubber, an absorber, and a reactor. Modeling this process accurately in ASPEN with a single tower would be difficult (if not impossible). This is not generally a problem because, as mentioned before, we can separate the different processes into individual ASPEN blocks and achieve satisfactory results. This procedure also gives the added benefit of independent inspection of each separate process individually. We can isolate problems and interesting results in individual processes much easier this way. We can come away from the simulation with more information because of this, although it remains under the caveat that the processes had to be separated. This separate treatment may or may not introduce error in the calculations.

We represent the scrubber/absorber (and reactor) as multiple blocks in ASPEN. At the bottom, we use two scrubber tanks (two-phase flash drums) to represent the scrubber section. At the top, we use a reactive absorption column to simulate the staged absorber. We incorporate the reactions in four stoichiometric reactors because reactions in the real process most likely run the whole height of the tower. We developed the arrangement of stoichiometric reactors within the scrubber/absorber by trial and error, comparing simulation results to RFAAP mass-balance data.

First, a reactor is placed in the liquid exiting the bottom scrubber tank (BOTREACT). This reactor simulates reactions occurring in the scrubber basin. A flash drum, downstream of this reactor, releases the vapors formed by the reactions back up to the scrubber (FLASHBOT). A second reactor is located in the liquid stream between the upper and lower scrubber tanks (SCRREACT). Thirdly, a reactor placed in the vapor stream between the top scrubber and absorber accounts for the initial contact between the fumes and the sprayed water (ABSREACT). Fourthly, a reactive absorption model simulates reactions on the absorber tower trays (ABSORBER). Table 3.8 summarizes the units we add to the ASPEN Plus simulation. These units account for behavior that the model units of the existing equipment could not.

Table 3.8. List of units added to ASPEN Plus simulation.

Unit (Block) Name	Purpose
ABSREACT	Gas-phase stoichiometric reactor
SCRREACT	Liquid-phase stoichiometric reactor
SCRUBTOP	Flash drum representing top scrubber stage
SCRUBBOT	Flash drum representing top scrubber stage
BOTREACT	Liquid-phase stoichiometric reactor representing scrubber basin
FLASHBOT	Flash drum representing scrubber basin (releases NO)

We must mention absorber stage efficiencies at this point. Stage efficiency refers to the degree to which vapor-liquid equilibrium is achieved on a stage. If we assumed

100% absorber stage efficiency, then our ASPEN Plus model of the absorber would have 16 trays, the same as the actual process. ASPEN Plus calculates absorber stgages as equilibrium stages. These are, by definition, 100% efficient. We must account for the inefficiency of real equipment, that is to say, the inability of most real processes to reach complete equilibrium. The typical empirical value for absorption tower efficiency is approximately forty percent (40%). Forty percent of 16 stages gives 6.4 theoretical stages. We use 7 stages for our ASPEN Plus model of the absorption tower. This number of theoretical trays translates to a tower efficiency of 44%.

ASPEN calculates the equilibrium for the HNO_3 dissociation reaction using the *Electrolyte NRTL* thermodynamic model. After specifying the components, ASPEN calculates the equilibrium for the HNO_3 dissociation reaction globally (in all blocks and streams). However, if we do not explicitly specify the dissociation reaction for the reactive-distillation column, ASPEN assumes the reaction does not occur in the column. ASPEN assumes this because all reactions in the column must be specified explicitly. This logic conflicts with and overrides the global specification of the reaction. Therefore, reaction (3.5), the HNO_3 dissociation reaction, must be specified in the ASPEN Plus reaction sheet along with the other reactions in the column,. Exemption of this reaction hinders the simulated performance of the column dramatically.

Primarily, we develop an accurate and robust computer model in ASPEN Plus by implementing simulation blocks and process variables within the simulation. After much trial and error, the successful model accurately simulates the available data representing

the true operational performance of the system. After establishing this working model, we incorporate adjustments in the process parameters of the computer simulation for the objective of process optimization. We observe the results of these process changes. For example, these process changes and the related results could include the positive effects of process optimization, or the negative effects to the system due to loss of process utilities (e.g., loss of cooling water flow to a reactor).

Next, we perform sensitivity analyses to determine the dependence of output variables on manipulated variables (e.g., the effect of column pressure on NOx concentration leaving the top of the column). ASPEN Plus can generate plots, called sensitivity plots, from the simulation data for a visual representation of these trends. Finally, we can simulate various competing retrofit and process optimization options on the computer. The model helps us assess the relative effectiveness and economic viability of the options. We know that the model behaves as the real system does before retrofit. We have confidence that the model accurately simulates how the system will behave after the retrofit options and changes in process variables are implemented. In this way, we can judge all these options based on the simulated performance of the process.

In this case, it becomes evident early on that the conversion model is not returning results consistent with the research we have done on how systems similar to the one at RFAAP respond to processing changes. Therefore, we present the results in the following sections of this chapter to prove this fact to the reader. The reader should note,

however, that this fact is not obvious without adequate research of the literature, because the model is accurate for the base-case data and for some minor process changes. However, the conversion model shows disappointing precision for changes in the most important factors affecting the NOx abatement processes. These factors should have yield dramatic changes in the results, but the conversion model erroneously shows them to be minimal.

3.4 Discussion of the Conversion Model Results

3.4.1 The Preliminary ASPEN Model

3.4.1.1 Scrubber/Absorber

For the model, we assume that reactions (3.3) and (3.4) predominate in the scrubber/absorber process. Through trial and error, we find fractional conversions for the reactions for the different stoichiometric reactors as shown in Table 3.9. The overall mass balance matches that of the data provided by RFAAP, but the set of fractional conversion values for individual stoichiometric reactors represents only one of many possible sets.

Table 3.9. Reactions in the scrubber/absorber and their percent conversion of the reactant shown.

Rxn #	Reaction Stoichiometry	Reactor Name/Location	Fractional Conversion	Key Reactant
3.3	$3NO_2 + H_2O \leftrightarrow 2HNO_3 + NO$	ABSREACT	0.83	NO_2
3.4	$2NO + O_2 \leftrightarrow 2NO_2$	ABSREACT	0.13	NO
3.3	$3NO_2 + H_2O \leftrightarrow 2HNO_3 + NO$	ABSORBER	0.1/tray	NO_2
3.4	$2NO + O_2 \leftrightarrow 2NO_2$	ABSORBER	0	NO
3.3	$3NO_2 + H_2O \leftrightarrow 2HNO_3 + NO$	SCRREACT	0.98	NO_2
3.4	$2NO + O_2 \leftrightarrow 2NO_2$	SCRREACT	0	NO
3.3	$3NO_2 + H_2O \leftrightarrow 2HNO_3 + NO$	BOTREACT	0.9	NO_2
3.4	$2NO + O_2 \leftrightarrow 2NO_2$	BOTREACT	0.9	NO

3.4.1.2 Demister

We represent the demister as a simple flash drum in the ASPEN model. Liquid exiting the bottom of the demister is sent to the drain. We have assumed a negligible amount of liquid entrainment at the top of the tower. Therefore, the ASPEN results show no flow to the drain.

3.4.1.3 Heat Exchangers and Process Heaters

We treat the preheater and the direct-fired heater as simple process stream heaters. ASPEN calculates the enthalpy change of the process streams for the specified temperature change. We can calculate steam or natural gas requirements from the amount of heat transferred to the process stream. The feed/effluent heat exchanger transfers heat from the process stream leaving the catalyst vessel (RECOUT) to the stream leaving the preheater (VAPOR). We treat it as a heat exchanger in the ASPEN model, specifying the outlet temperature of the hot stream (RECOUT). Table 3.10 outlines the temperature change and heat duty that the individual heating units incur on the process streams involved.

Table 3.10. Stream temperature changes and heat duties for the heat exchangers and process heaters.

Process Stream	Equipment Name	ASPEN Desig.	Inlet Temp., ^{o}F	Outlet Temp., ^{o}F	Heat Duty, BTU/hr
FLASHOUT	Preheater	PREHEAT	80	100	543563
VAPOR	Economizer	HEATX	100	357	1384333
RECOUT	Economizer	HEATX	600	350	-1384333
VAPOROUT	Direct-Fired Heater	DIRHEAT	357	600	506077

3.4.1.4 Catalyst Vessel

As in the scrubber/absorber, we chose fractional conversions to accurately match the operating data for the SCR. Table 3.11 shows the important reactions and the percent conversion of ammonia (NH_3) feed.

Table 3.11. Reactions in the catalyst vessel and their percent conversion of the reactant shown.

Rxn #	Reaction	Fractional Conversion	Key Reactant
3.6	$4NH_3 + 6NO \leftrightarrow 5N_2 + 6H_2O$	0.56	NH_3
3.7	$4NH_3 + 4NO + O_2 \leftrightarrow 4N_2 + 6H_2O$	0.06	NH_3
3.8	$2NO_2 + 4NH_3 + O_2 \leftrightarrow 3N_2 + 6H_2O$	0.26	NH_3
3.9	$NO + NO_2 + 2NH_3 \leftrightarrow 2N_2 + 3H_2O$	0.12	NH_3

Table 3.12 gives the outputs of the system as calculated by ASPEN (simulation results) as compared to the mass balance provided by RFAAP (RFAAP data). We show numbers of key interest in bold. We bring the reader's attention to the disparity between the molar flow rate of water in the waste-acid stream (WASTACID). This disparity results because we believe the value provided by RFAAP for the water content of this stream to be erroneous. With 22.17 lbmol/hr (399.4 lb/hr) of filtered water fed into the top of the absorber, for 13.1 lbmol/hr (236.1 lb/hr) to emerge at the bottom, 9.07 lbmol/hr (163.4 lb/hr) must evaporate and be carried with the gas stream inside the

scrubber/absorber. The fume stream should be nearly saturated with water vapor before it enters the absorber. In addition, the fume stream cools somewhat within the column (from 90 ^{o}F to approximately 80 ^{o}F). Therefore, it is unlikely to cause the evaporation of that much water.

Table 3.12. Output flows as calculated by ASPEN compared to those supplied by RFAAP.

Stream: Mole Flow Lbmol/hr	WASTACID (Simulation Results)	Acid From Scrubber (RFAAP Data)	PRODUCT (Simulation Results)	Gas to Vent Stack (RFAAP Data)
NO	9E-3	-	**0.06**	**0.06**
NO_2	6E-3	-	**9.7E-3**	**trace**
NH_3	-	-	**0**	**trace**
O_2	1.7E-6	-	132.1	132.06
N_2	1.7E-6	-	498.8	496.8
H_2O	**21.4**	**13.1**	15.9	23.9
H_2SO_4	-	-	-	-
HNO_2	-	-	-	-
HNO_3	2.091	2.1	-	-
Total Flow lbmol/hr	25.6	20.8	646.8	654.8
Total Flow lb/hr	556	376	18487	18631
Total Flow cuft/hr	7.8	-	3.9E5	-
Temperature F	80	86	350	350
Pressure psi	**14**	**60**	14.4	14.1

Though the model accurately simulates the system, the assumptions inherent in this configuration could create some problems in future modeling. For example, the incorporation of multiple stoichiometric reactors may not adhere to the true mechanism of the reactions. We simply do not know where the reactions take place. Specifically, all the reactions could occur in the bottom of the scrubber section, or each reaction could occur in different phases or locations in the column. Most likely, however, the reactions occur throughout the column. The conversion model, however, gives us no information in this area, because we have specified the reactions to take place in the sections where the reactors are placed. This fact becomes noteworthy when considering the information on the reactions given by the equilibrium model. We shall discuss this information and its accuracy in the following chapter.

The assumption of stoichiometric reactors most obviously becomes a problem when we change the number of stages in the simulation of the column. In that case, fewer stages would definitely reduce the separation performance. Also the effective reduction in volume of the absorber as a reaction vessel would decrease the conversion of NOx gases to nitric acid, further increasing the NOx gases to escape out the top. Obviously, increasing the number of stages has the opposite effect.

Modeling the absorber with reactive absorption reduces the potential for error, but we have assumed a conversion factor on the stages that may vary with true conversion. This problem warrants further study of the reaction mechanism for accurate modeling of design changes. The reader should note that we neglected reactions 2 and 3 in Table 3.1

altogether. We choose the conversions for reaction to match the operating data for the scrubber/absorber. With these conversions, our simulation matches the mass-balance data given by RFAAP. Initially, the reaction conversions shown in Table 3.9 may seem to be an arbitrary selection for reaction conversions. However, since the real process must adhere to the conservation of mass, the overall conversion in the model matches well with the running data provided by RFAAP. This accurate match should lend confidence to the assumptions made above for the overall mass balance. The question remains where the reactions tend to occur and whether these assumptions will affect further sensitivity tests and retrofit analyses using the model. We state the potential problems with the assumptions for the sake of completeness and for insight in the event of further research into the absorption process.

3.4.2 Absorption-Column Performance

The performance of the NOx abatement system hinges on the performance of the scrubber/absorber column and the catalyst vessel itself. This section of this report covers the performance of these two key units in greater detail. The absorption column accounts for most of the removal of the total NOx gases (on a mass basis) fed to the system. Also, the reactions in the column set up the production of NO at the expense of NO_2. Although it possesses some potential for NO_2 reduction, the catalyst vessel is designed primarily to reduce NO with ammonia. Therefore, satisfactory performance of the catalyst vessel hinges on the desired output from the absorption column.

Figure 3.19 shows the profile of the absorption column in temperature and pressure on each stage as calculated by ASPEN. The temperature gradient would have a definite effect (though to an undetermined extent) on the reaction rate in treating the reactions rigorously. We specify the pressure profile by giving a pressure drop per stage in ASPEN. The temperature on each stage is calculated by ASPEN from the thermodynamic model.

Figure 3.20 shows the performance of the absorption column with respect to the reduction of NOx vapors as calculated by ASPEN. The figure clearly shows that NO is negligibly soluble in water. NO is enriched in the vapor towards the top of the column. The column also tends to enrich NO_2 toward the top stage. However, the combined effect of consumption of NO_2 by reaction results in a net decrease in NO_2 in the liquid and vapor up the column.

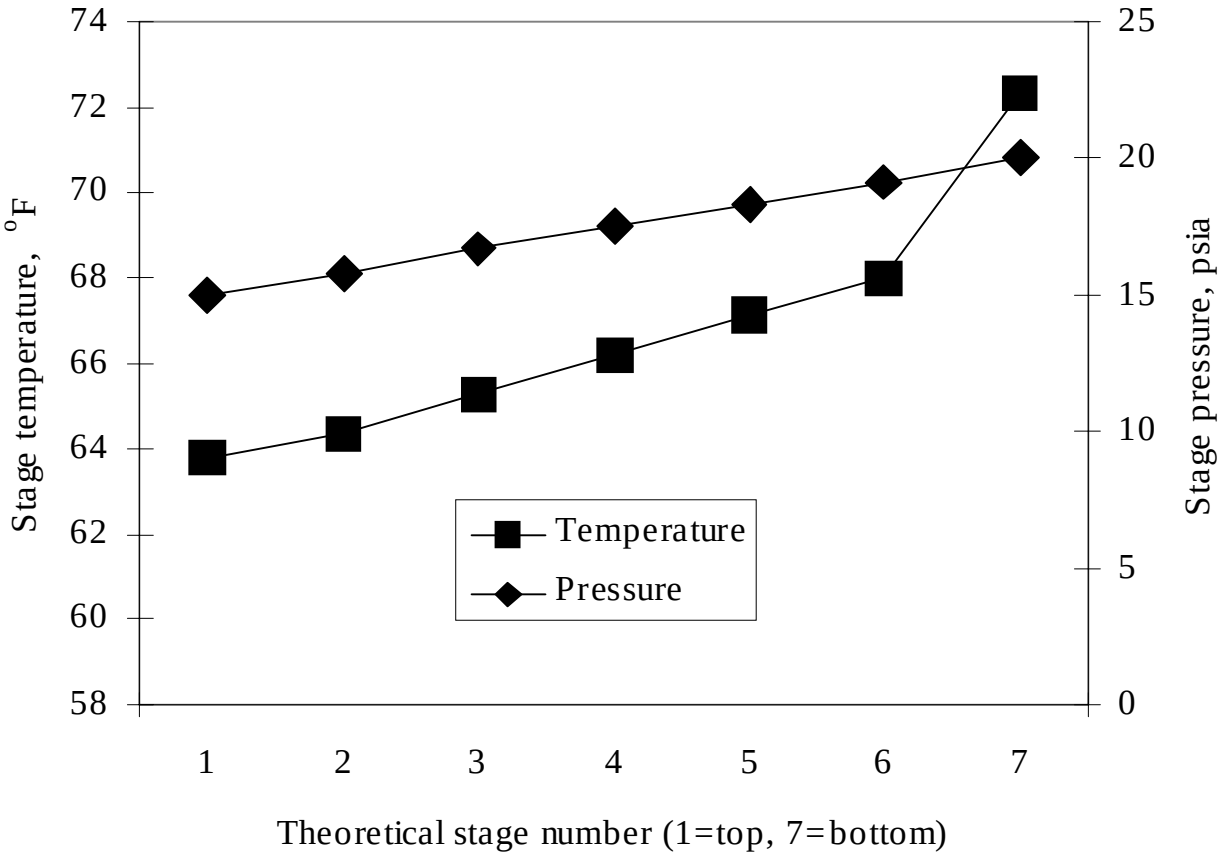

Figure 3.19. Temperature and pressure profile for the simulation of the absorption tower. The abscissa corresponds to the theoretical stages in the ASPEN model. ASPEN numbers column stages from top to bottom. Stage 1 corresponds to the top stage (stage 1) in the real column, and stage 7 here corresponds to the bottom stage (stage 16) of the real column.

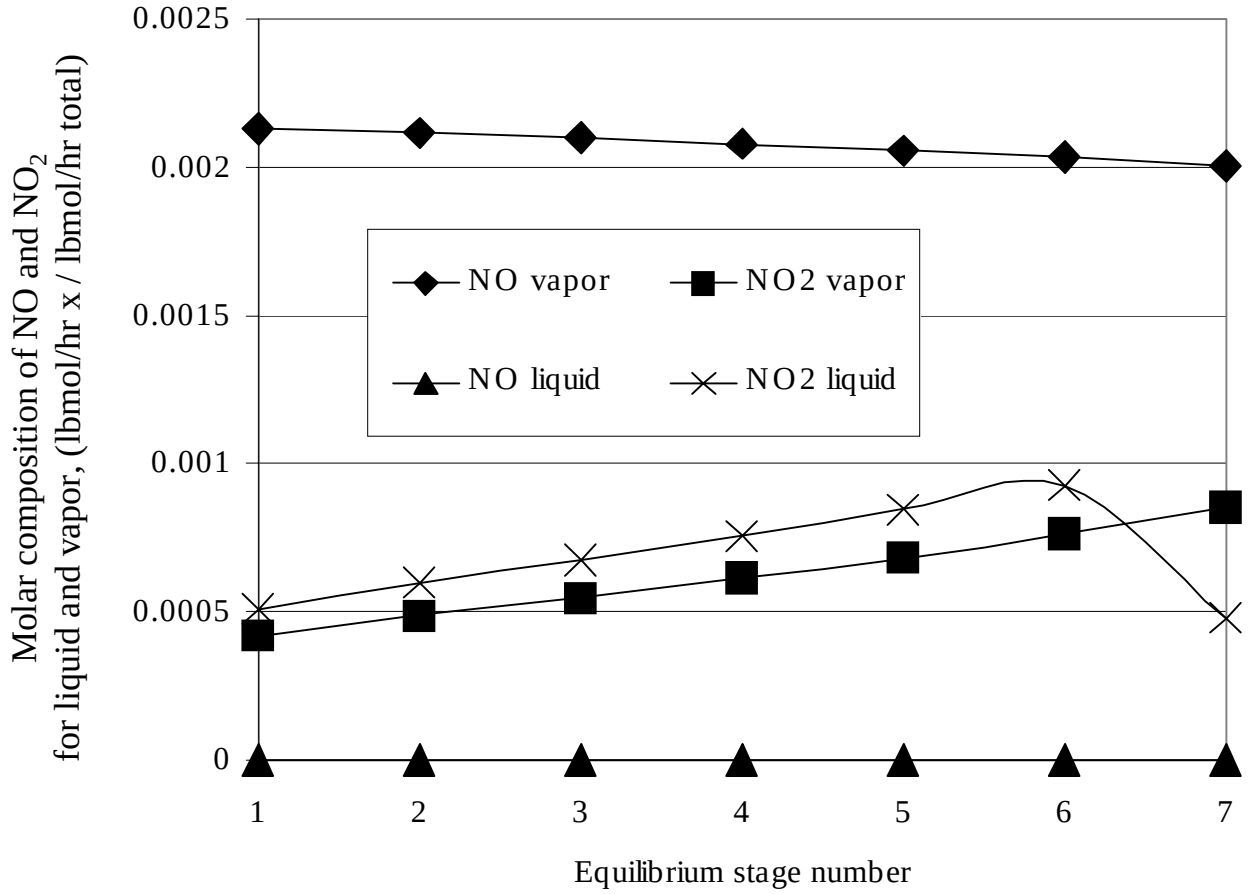

Figure 3.20. Absorber column profile for molar compositions of NO and NO_2. Figure shows the liquid and vapor on the theoretical absorber stages. Stage 1 is the top stage, and stage 7 is the bottom stage.

Cheremisinoff and Young (1977) present work concerning scrubber performance for the removal of NO_2. They show that scrubber performance, measured by percent removal of NO_2, decreases with increasing temperature, decreasing NO_2 concentration, and increasing gas flow rate. From the data by Cheremisinoff and Young, we have constructed a theoretical stage profile for NO_2 concentration for the scrubber/absorber. Figure 3.21 compares the data from Cheremisinoff and Young to that calculated by the conversion-model simulation.

We clearly see that the conversion fits the general trend of the experimental data. The conversion model qualitatively mimics the dramatic NOx removal in the scrubber section of the scrubber/absorber tower. The removal levels off higher up the column. However, the NO_2 levels drop too steeply in the scrubber and levels off too much in the absorption tower. This results from the arbitrary nature of the percent conversion specifications for the reactions within the model. The data by Bowman et al. clearly show that the driving force for NO_2 removal decreases as more and more NO_2 is removed. The same trend results in the conversion model by sheer serendipity.

We choose the percent conversion in ABSREACT as 0.83 knowing that the bulk of NO_2 would likely be removed where the concentration is highest. The percent conversion we choose for the absorption trays in ABSORBER is 0.1 per tray by reaction (3.3). These factors are not functions of the initial NO_2 concentrations as they are in reality (reaction rates depend on concentrations). Figure 3.22 shows the problem that

results from the omission of this capability from the conversion model. The data by Bowman et.al. give a much more realistic curve. We see the overly dramatic NO_2 removal of the conversion model scrubber section seen here. Again, we see the same general trend for the conversion model as with the experimental results. However, the NO_2 removal is overly optimistic and does not change enough with respect to inlet NO_2 concentration. We could possibly have lived with this lack of accuracy if the model proved precise for conditions used for optimization. As we will show later, that is not the case.

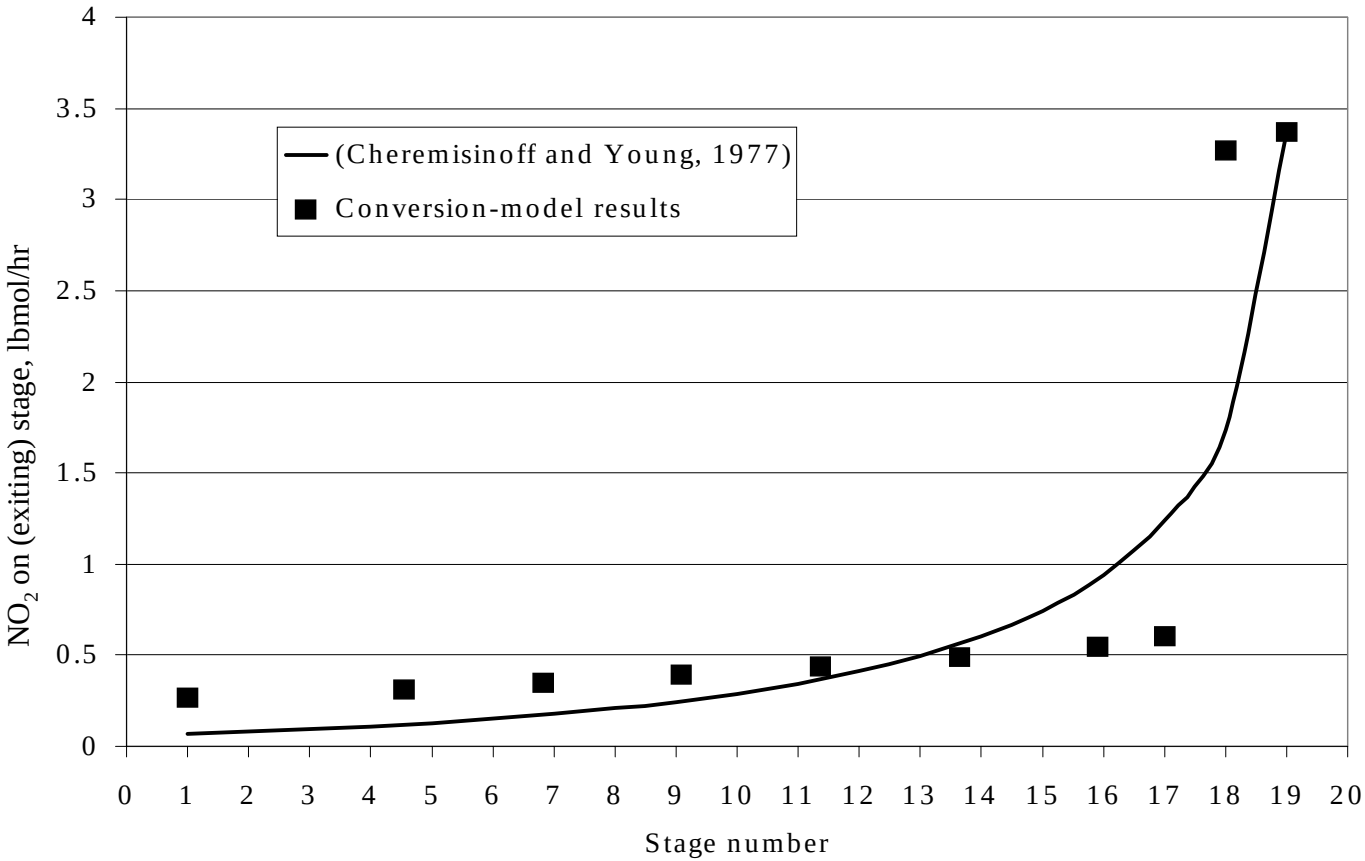

Figure 3.21. Scrubber/absrober column profile for NO_2 flow rate. Stage 1 represents the top tray of the absorption column, stage 16 the last bubble-cap tray. Stage number 17 represents the upper scrubber stage (SCRUBTOP). Stage 18 the lower scrubber stage (SCRUBBOT). Stage 19 represents the fumes fed to the column.

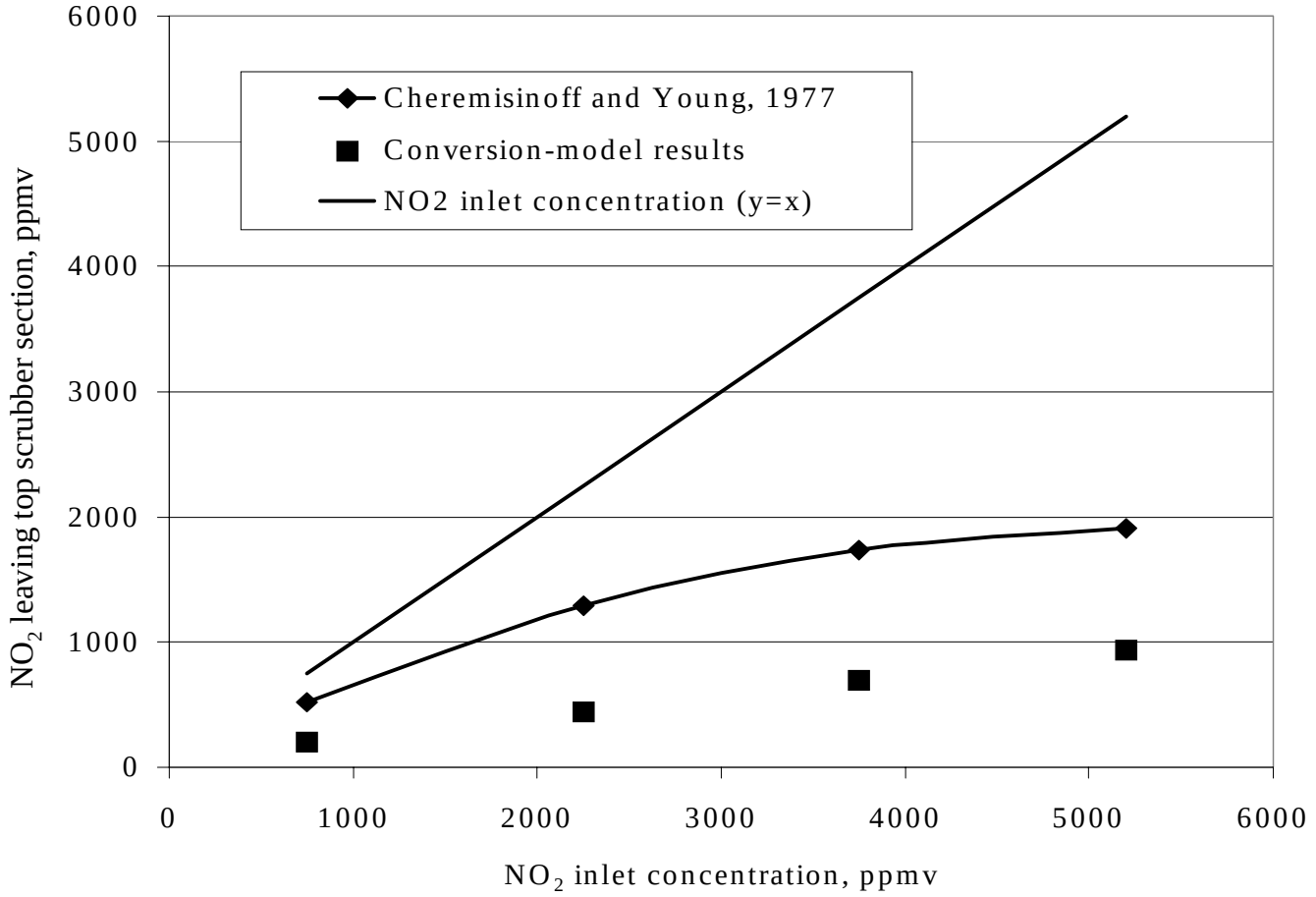

Figure 3.22. Comparison of conversion-model results to those presented by Cheremisinoff and Young (1977). We show the y = x line (in = out) to simplify comparison of the two data sources. The conversion model gives optimistic results for NO2 removal. Also, the removal rate does not vary with inlet concentration to the degree that the experimental results do.

3.4.3 Sensitivity Analysis

We alluded in Chapter two what the experimental literature has found to be the most important process variables for NOx absorption and SCR. In the previous sections, we have seen that the conversion model, though not perfect, follows the general trends expected for the processes of NOx absorption and SCR. The question must be answered as to whether or not we can accept the inaccuracies of the model and move on, using it as a process optimization and prediction tool. We have alluded to the fact that we could not. The following figures and explanation show that the conversion model cannot predict responses to the most important process changes as compared to the experimental and theoretical literature.

3.4.3.1 Fume-Feed Temperature

We treat the scrubber drums in ASPEN as adiabatic units. Therefore, the fume-feed temperature determines the scrubber temperatures for the most part. Filtered water temperature, and heats of reaction and absorption have minimal effects on temperature. We can ignore these small effects as negligible and equate fume-feed temperature with scrubber temperature. Reducing the NOx absorption temperature aids in absorption in nearly all aspects. We predict that reducing the fume-feed temperature, as a means of reducing absorption temperature, to have a dramatic effect for improving NOx

absorption. If the conversion model can predict this behavior, we should see reductions in NOx escaping the top of the column, as well as an increase in nitric acid leaving the bottom, for each successively lower temperature.

Figure 3.23 illustrates the comparison between what the literature predicts for the effect of process temperature on NOx absorption to the results obtained from the conversion model. Clearly, the model does not react to temperature in the manner that the literature predicts should be the case. This follows because of the constant reaction conversions and the equilibrium-stage calculation approach of ASPEN for the simulation. With constant reaction conversions, temperature does not alter the ratio of reactants that get changed to products in the stoichiometric reactors. With the equilibrium approach to the calculation of vapor-liquid equilibrium, the rate of absorption never enters into the calculations. Therefore, if temperature affects the equilibrium of absorption moderately, but the rate of absorption greatly, an equilibrium model will underestimate the effect. With the inability to predict response to temperature, we show a major shortcoming of the conversion model.

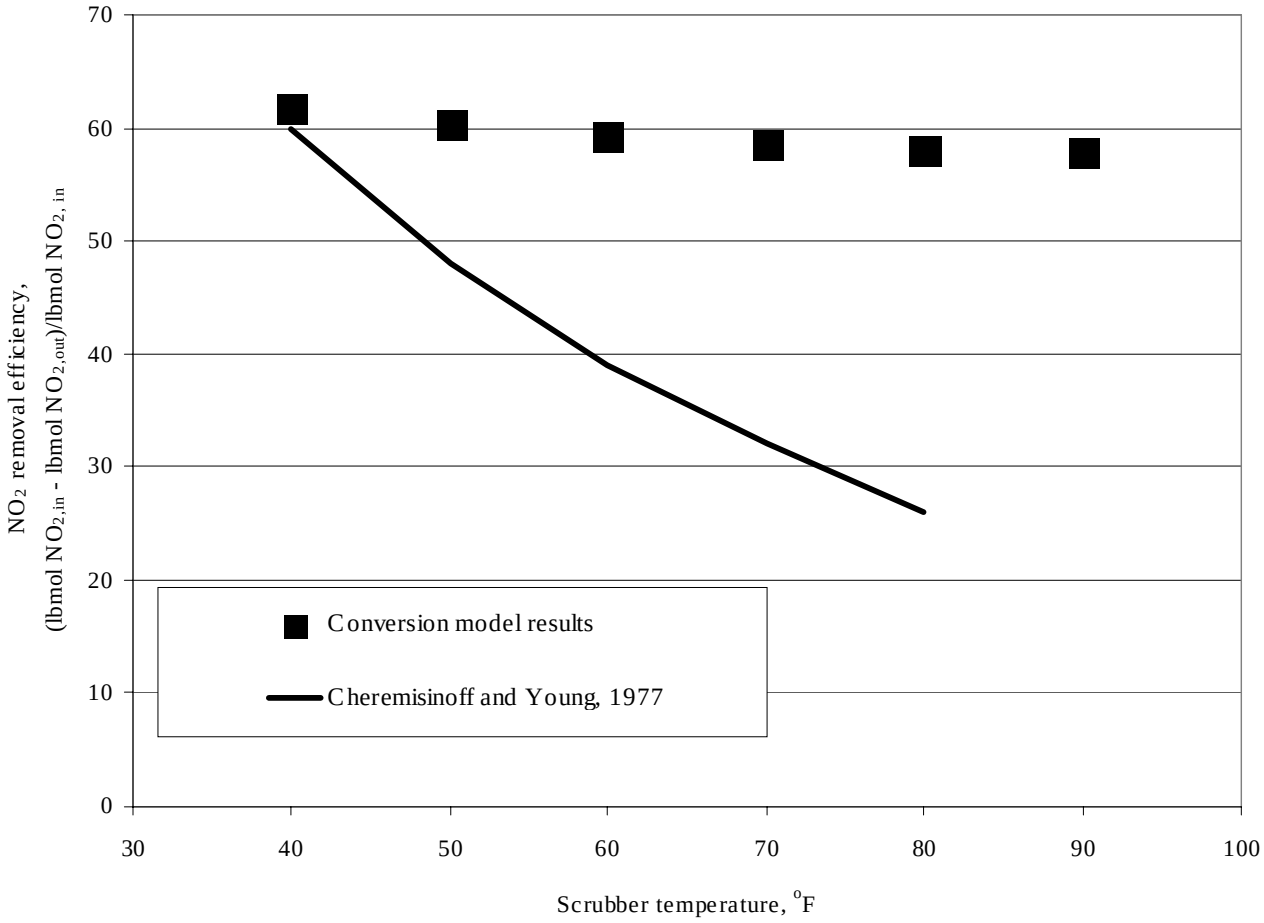

Figure 3.23. Sensitivity plot of the effect of scrubber temperature on NO_2 removal efficiency.

3.4.3.2 Top-Stage Pressure

We have specified a constant pressure drop per stage for the absorption column. Specification of the top-stage pressure of the absorption column, therefore, determines the pressure throughout the rest of the column. Experimental results have shown that NOx absorption is strongly dependent on the pressure of the process. Figure 3.24 shows the effect of scrubber/absorber pressure on NO_2 escaping the top of the column and HNO_3 leaving in the waste-acid stream.

3.4.3.3 Water Flow rate

Increasing the flow rate of filtered water provides the NOx with more "room" to absorb. Also, for certain temperature, pressure, and NOx concentrations, there exists a maximum nitric acid concentration above which no further NOx will absorb. Obviously, running higher water flow rates dilutes the nitric acid and allows more NOx to absorb. Again, the stoichiometric reactors do not take this phenomenon into account when calculating the reaction conversion. Therefore, we predict increasing the filtered-water flow rate will have little effect on the NOx removal efficiency. Figure 3.25 shows the effect of scrubber temperature on the NO_2 removal efficiency.

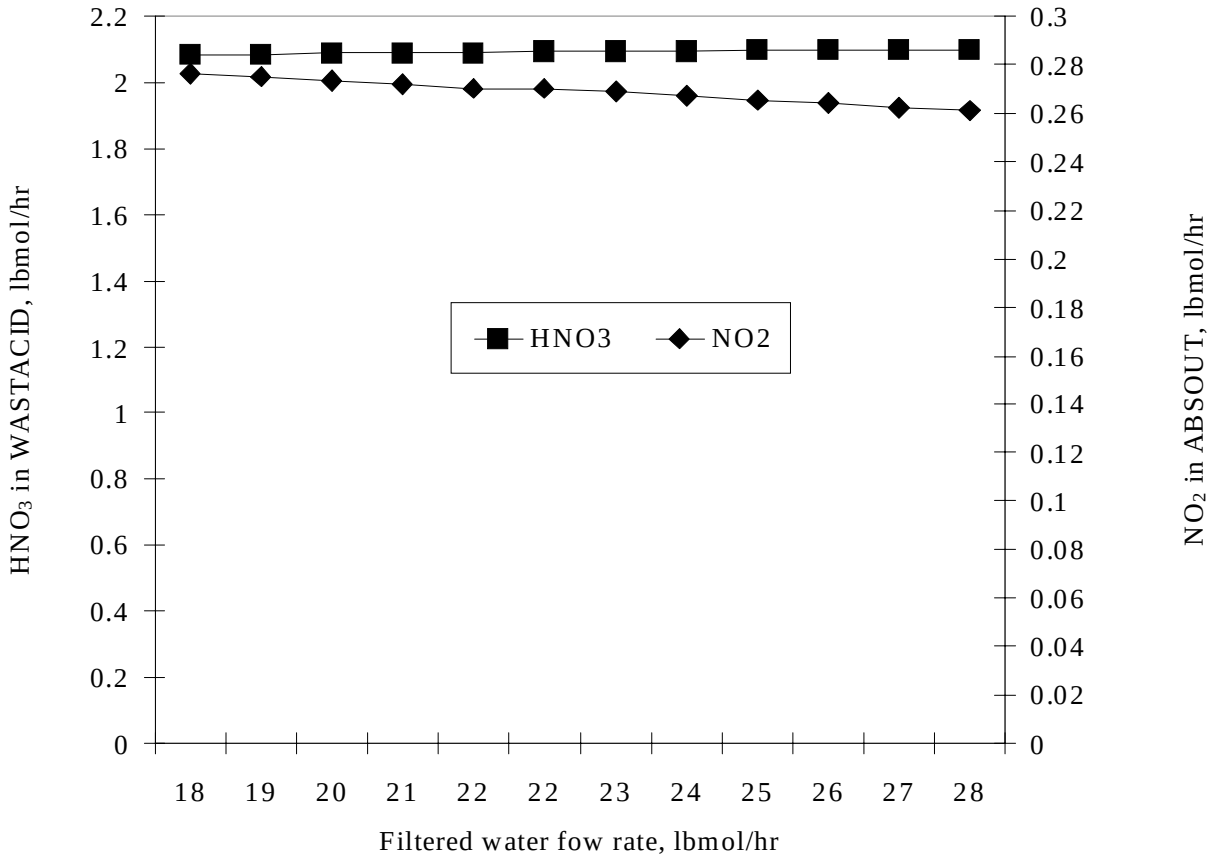

Figure 3.24. Sensitivity plot of the effect of filtered water flow rate on NO_2 and HNO_3 leaving the scrubber/absorber.

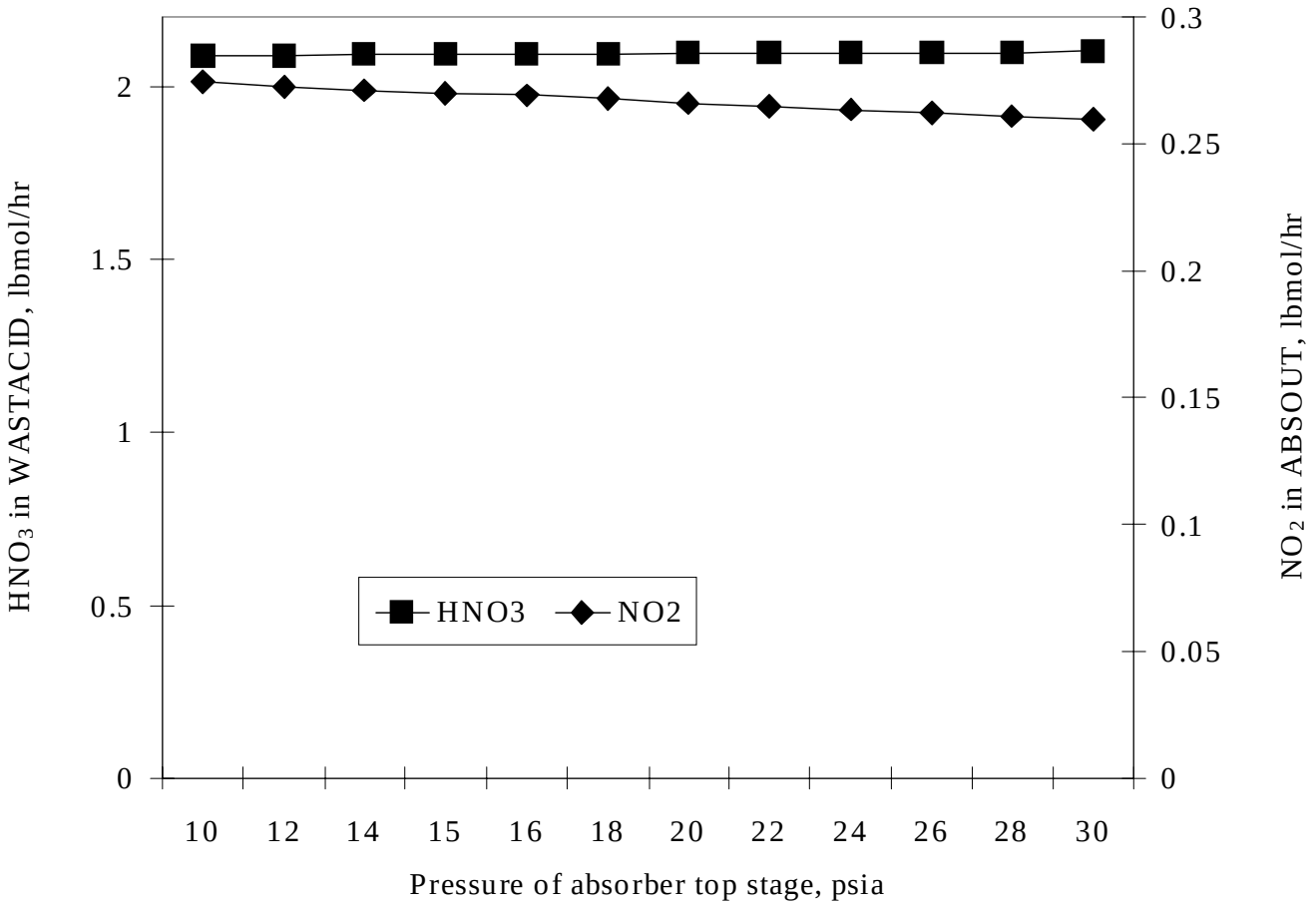

Figure 3.25. Sensitivity plot of the effect of scrubber/absorber pressure on NO_2 and HNO_3 leaving the scrubber/absorber.

3.5 Conclusions

3.5.1 Conclusions Regarding Process Variables

We have seen that certain process variables strongly affect the absorption efficiency of NOx. The conversion model corroborates the evidence presented from the literature qualitatively in that the general trends are repeated therein. However, the degree to which the literature predicts that the absorption should be affected does not appear in the conversion-model simulation results. We have explained that this stems from the constant reaction conversions of the model.

Although this conclusion represents a limitation of the conversion model, it also gives a very important bit of information concerning NOx absorption. A revelation of supreme importance is that reactions take in the process of NOx "absorption." In other words, the process of NOx removal by absorption or scrubbing must be approached as more of a reaction engineering problem than that of simple mass transfer. Reactions determine the total amount of NOx absorbed and, to a lesser extent, the rate at which NOx can be absorbed.

Approaching NOx absorption as a reaction network makes clear some of the advantages that can be gained from certain process variables that are usually ignored when dealing with typical absorption and scrubbing processes. Temperature, for

example, takes a secondary role in most absorption processes. However, in the case of NOx absorption, it has a surprisingly dramatic effect.

The domination of reaction makes inconsequential some of the key variables usually associated with optimization of these same processes. For example, nitric acid concentration hinders NOx absorption relatively little up to almost 35% acid by weight. In fact, it is theorized that nitric acid can improve NOx absorption under some circumstances. For most absorption processes, increasing the driving force for mass transfer requires a low liquid concentration of the component being absorbed. This is not necessarily the case in NOx absorption.

3.5.2 Problems with the First Equilibrium Model

As stated above, the main failure of the conversion model arises from the inability of constant reaction conversions to adjust to process variables that, in reality, have dramatic effects on reaction rates and equilibria. This situation manifests itself in reduced responses to changes in these process variables than we observe in the actual process. We have discussed some of the more important variables in this chapter. We arrived at several conclusions regarding the conversion model.

1. The conversion model yields errors of almost 100% compared to literature predictions for the ratio of NO_2 fed to that removed as in Figure 3.22.

2. The conversion model gives disappointing results for the effect of filtered water flow rate on NOx removal efficiency as seen in Figure 3.23.

3. The conversion model fails to predict the effect of column pressure on NOx removal efficiency as seen in Figure 3.23.

4. The response of NO2 absorbed in the scrubber for changes in temperature is an order of magnitude lower than that of experimental results presented by Cheremisnoff and Young (1977) for a similar process.

5. The response of the NOx absorption system is consistent with those displayed by mass-transfer-only processes where reaction is not encountered.

3.6 Recommendations

1. Use a conversion model for creating a mass balance and for judging the effect of process variables on the mass-transfer aspects of the process.

2. Explore the use of column-cooling techniques for new and existing NOx absorption processes.

3. Feed NOx in as undiluted a form as is feasible.

4. Increase column pressure for increased NOx removal and viable acid recovery.

5. Increase filtered-water flow rate for increased NOx removal and decrease flow rate for increased acid concentration.

6. Exercise strict control of ammonia injection to a selective catalytic reduction reaction vessel.

3.8 Nomenclature

atm	atmospheres of pressure
DEQ	Department of Environmental Quality
lbs/hr	pounds per hour, mass flow rate
kPa	kilopascals of pressure
NRTL	non-random two-liquid thermodynamic model
NC	nitrocellulose
ppmv	parts per million by volume
PSIA	pounds per square inch (absolute) of pressure
scfm	standard cubic feet per minute, volumetric flow rate
tons/yr	tons per year

3.9 References

Cheremisinoff, P. N., and R. A. Young, R. A., Ed., *Air Pollution Control and Design Handbook, Part 2*, Marcel Dekker, Inc., New York (1977), pp. 628, 671.